VIBRATION OF AN AXIALLY MOVING CURVED WEB

BY

AALIM MOTASIM AALIM MUSTAFA

A Thesis Presented to the

DEANSHIP OF GRADUATE STUDIES

KING FAHD UNIVERSITY OF PETROLEUM & MINERALS

DHAHRAN, SAUDI ARABIA

In Partial Fulfillment of the
Requirements for the Degree of

MASTER OF SCIENCE

In

MECHANICAL ENGINEERING

May 2015

KING FAHD UNIVERSITY OF PETROLEUM & MINERALS

DHAHRAN- 31261, SAUDI ARABIA

DEANSHIP OF GRADUATE STUDIES

This thesis, written by **AALIM MOTASIM AALIM MUSTAFA** under the direction of
his thesis advisor and approved by his thesis committee, has been presented and accepted
by the Dean of Graduate Studies, in partial fulfillment of the requirements for the degree
of **MASTER OF SCIENCE IN MECHANICAL ENGINEERING**

Dr. Zuhair Gasem

Department Chairman

Dr. Salam A. Zummo
Dean of Graduate Studies

29/2/16

Date

Dr. Muhammad Hawwa
(Advisor)

Dr. Abdelaziz Bazoune
(Member)

Dr. Mehmet Sunar
(Member)

Dedication

To my family

ACKNOWLEDGMENTS

TABLE OF CONTENTS

LIST OF TABLES

LIST OF FIGURES

LIST OF ABBREVIATIONS

A	Area of the beam cross section
b	Width of the beam
c	Dimensionless speed of the beam
E	Modulus of elasticity of the beam
h	Thickness of the beam
I	Inertia of the beam
k_1	Linear stiffness of the path supports
k_2	Nonlinear stiffness of the path supports
L	Length of the beam
P	Applied tension
q	Time function for transverse vibration
T	Kinetic energy
U	Strain energy
v	Axial speed of the beam
v_1	The longitudinal stiffness of the beam
v_f	The flexural rigidity of the beam
w	Transverse vibration

ω	Frequency of beam vibration
Z	Path curvature function
e	Amplitude of path curvature
μ	Viscous damping coefficient
$\emptyset$	First mode shape of the beam
F	Applied external force
Ω	Frequency of the External force
C^*	Critical speed of the beam

ABSTRACT

Full Name   : [AALIM MOTASIM AALIM MUSTAFA]

Thesis Title   : [VIBRATION OF AN AXIALLY MOVING CURVED WEB]

Major Field   : [MECHANICAL ENGINEERING]

Date of Degree : [May 2015]

This thesis presents a study on vibration of an axially moving web following a curved path. The web is considered as a simply supported beam travelling axially on a curved guide that consists of a combination of linear and nonlinear elastic supports. The main objective of this work is to investigate the effect of the path curvature on the moving beam vibration and investigate the effect of different parameters on the system's dynamic response. These parameters include axial speed, applied tension, degree of curvature of the path and stiffness of the path supports. The Galerkin decomposition with a first mode-shape of a straight a pinned-pinned basis function is utilized to realize a mathematical model that describes the static and dynamic behaviors of the axially moving curved beam.

Numerical solutions of the developed model are obtained using a fourth-order Runge-Kutta algorithm under MATLAB environment. Fundamental frequencies are calculated results for axially moving curved beams and compared with those for axially moving straight beam. Amplitude-frequency curves are developed to study forced vibration of the axially moving curved beam under an external force excitation. Poincaré sections and bifurcation diagrams are obtained for three cases: primary, sub-harmonic, and super-harmonic resonance excitations. It is found that the natural frequency of an axially moving beam

travelling on a curved elastic support is higher than that of its axially moving straight beam for all considered cases of different path curvatures and different degrees of support stiffness. Forced vibrations of an axially moving beam on a curved elastic support are considered under harmonic excitation. Using the excitation amplitude as a controlling parameter over a wide range of variation, while keeping the excitation frequency fixed, it is found that the system exhibits many types of bifurcations, including period doubling bifurcation, period four bifurcation and many jumps. Compared to an axially moving beam resting on a straight elastic support, the axially moving curved beam showed earlier bifurcation and more swarming bifurcation diagram.

ملخص الرسالة

الاسم الكامل: عالم معتصم عالم مصطفى

عنوان الرسالة: اهتزاز جائز منحني متحرك أفقيا

التخصص: الهندسة الميكانيكية

تاريخ الدرجة العلمية: مايو 2015

هذا البحث يعرض دراسة على لوح متحرك أفقيا يتبع مسار منحني. اللوح اعتبر على أنه جائز مرتكز على دعامات بسيطة، و يتحرك أفقيا على مسار منحني مكون من نابض خطي ولا خطي. الهدف الأساسي من هذا البحث هو دراسة تأثير الانحناء على اهتزاز الجائز المتحرك و دراسة تأثير عوامل مختلفة على استجابة النظام. هذه العوامل هي: السرعة المحورية ، الشد على الجائز ، انحناء المسار و صلابة النابض. تم استخدام طريقة جالركين للشكل الأول لاهتزاز جائز مرتكز على دعامات بسيطة كدوال أساسية لأشتقاق المعادلة الحاكمة للجائز التي تصف سلوك الجائز المتحرك أفقيا على مسار منحني.

تم إيجاد الحل العددي للمعادلة الحاكمة باستخدام خوارزمية رنج-كتا في برنامج ماتلاب. تم حساب الترددات الأساسية للجائز المتحرك فوق مسار منحني و تمت مقارنة النتائج مع حالة الجائز المتحرك على استقامة. تم الحصول على منحنيات قيمة الذروة – التردد لدراسة اهتزاز الجائز تحت تأثير قوة خارجية. تم الحصول على مخططات بوانكاريه ومخططات التفرع لثلاث حالات: الرنين الأساسي و مضاعفات الرنين العليا والصغرى. وجد أن التردد الأساسي للجائز المتحرك فوق مسار منحني أكبر من التردد الأساسي لنقيضه المستقيم لكل قيم انحناء المسار و صلابة النابض. تم اعتبار القوة الخارجية على أنها إثارة توافقية. بتثبيت تردد القوة الخارجية و التحكم في اتساع القوة الخارجية في مدى محدد تم إيجاد مخططات تفرع ثنائية، رباعية و عدد من القفزات. مقارنة مع الجائز المتحرك على دعامة مستقيمة لوحظ أن الجائز المتحرك فوق مسار المنحني يتعرض لحصول تفرعات في زمن أسرع ، وتكون أشد كثافة.

CHAPTER 1

Introduction

1.1. Motivation

In roll-to-roll (R2R) systems, flexible materials can be transported on rollers under or through processing machinery where processing operations, such as stamping, printing, coating, sputtering, etc., are performed to obtain a finished product. Figure 1.1 shows a R2R system with chemical processes on a moving substrate (web).
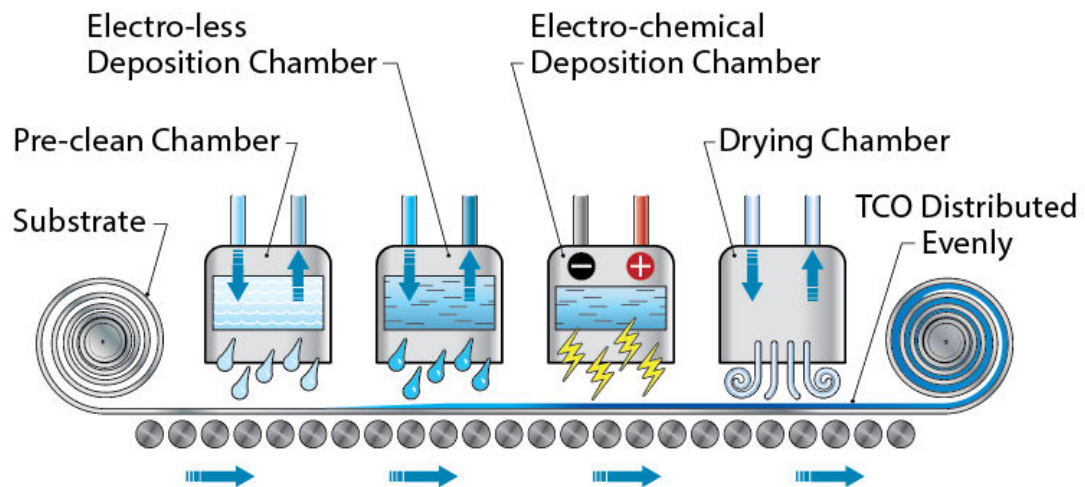
Figure 1.1 Different process on a moving substrate [1]

Figure 1.2 shows a casting process for copper based bi-metal strips. The blue box in the figure illustrates three processes performed on the moving metal sheet.
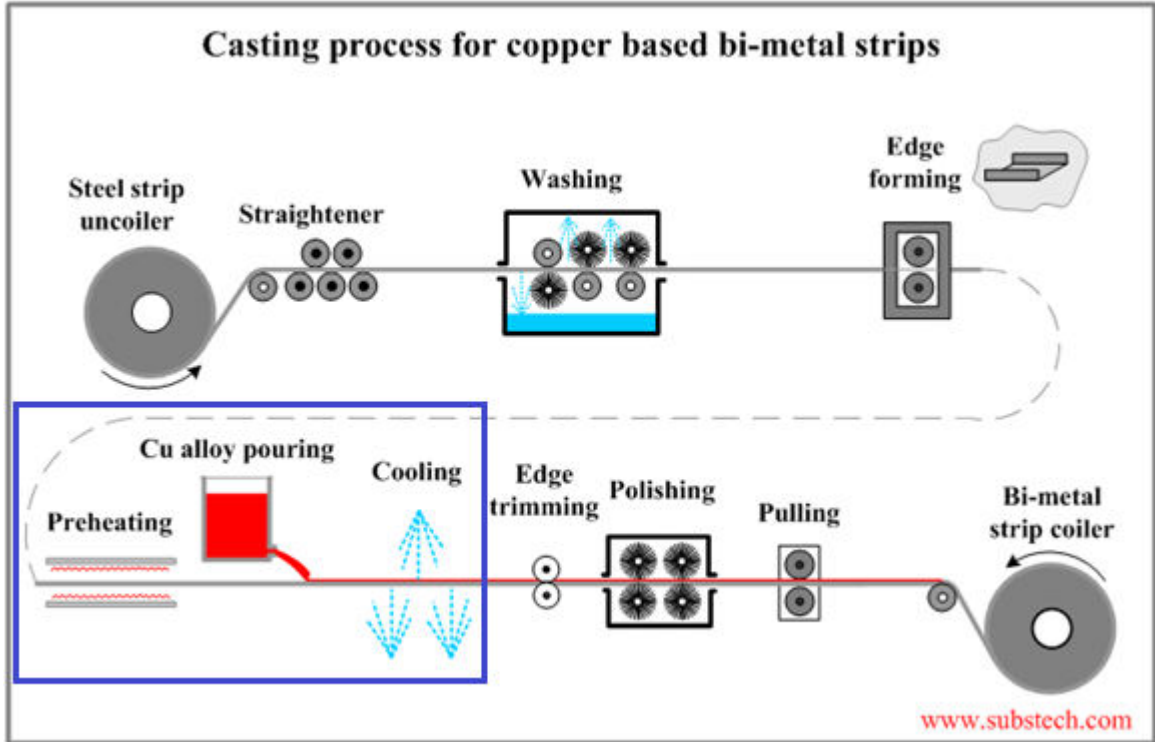
Figure 1.2 Casting process for moving copper based metal [2]

In case of straight web, the moving web is supported only by two rolls at the ends, the process is likely to be accomplished with low quality. Vibration of the web can be caused by the force applied from a certain process in the transverse direction.

Supporting the web in the domain between rolls can stabilize the moving substrate. If the support between the rolls is made curved (concave or convex), it allows more web processing capabilities compared to the straight support. In this thesis, we consider the case

of making a moving web to follow a curved path defined by intermediate support of the web when performing different industrial processes.

The idea of using curved intermediate support may also be effective if the span between the rolls is long, which could make the web to be subjected to wrinkling. Especially, in case of thin webs such as paper webs or sheet metallic web applications, as shown in Figure 1.3.
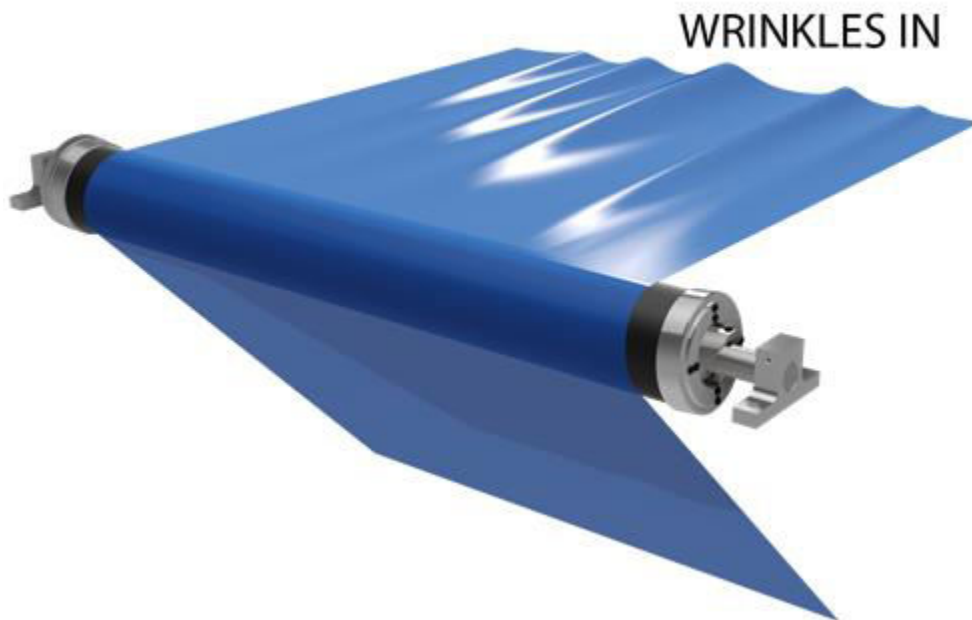
Figure 1.3 Wrinkles in paper web [3]

Furthermore, applications of axially moving webs resting on curved intermediate support is applied in fitness equipment. Figure 1.4 shows Wood-way® Curve treadmill which is a non-motorized treadmill powered solely by user's legs.

A quote from the manufacturer states: " The difference between a regular treadmill and the new curved design is that, in curved powerless treadmills the user have to be the power of the machine, so he is utilizing more muscles, making the whole effect more like running outside" [4].

Figure 1.4 Wood-way Curve treadmill [4]

1.2.   Roll to Roll Systems

In the last decades, there have been many applications which employed roll-to-roll (R2R) technology for mass production in applications such as power transmission belts, plastic films, chain drives, high speed magnetic tapes, paper sheets under processing, and steel strips. In many of these processes, the web motion can be modeled in the form of axially moving structural components. In these systems, the application of roll-to-roll processing yields better performance and supports mass production and high speed automation. The regions where material has to pass over a free span, without additional support, (e.g. between two rolls), are particularly interesting. These are the positions where system's dynamic could cause quality problems or even web breaks, because of high vibration amplitudes.

In R2R systems, mechanical vibrations (particularly in the transverse direction) of web materials between rolls have been a main quality and productivity limiting factor. If the vibration amplitude becomes sufficiently large or its excitation frequency matches the eigen frequencies of the web, it may result in excessive vibrations. Material failure due to excessive vibration wastes product and time, limiting the process productivity. Since the quality requirement as well as productivity in a production line is a key factor, Active vibration reduction has the potential to greatly increase process productivity by eliminating vibration-induced process failures. In axially moving systems, the transverse vibration of the moving web often causes a serious problem in achieving good quality.

Vibrations are inevitable in every complex machine that has many moving parts. In R2R systems there are many sources of vibration, e.g., roller eccentricity, tension variations, irregular speed of the driving motor, web-roller adhesion, defective bearings, vibration of the press foundation and environmental disturbances [5] .

It is significantly important to control the tension and the speed in the web feeding. A tension control system of moving web is inherently sensitive to external disturbances during operation, and the time-varying torque of the driving motors can cause severe tension variation. According to actual working conditions, the tension control system may be subjected to many uncertainties, such as a periodic disturbance from the eccentricity of the driving pulley, a time-varying radius of the unwinding/rewinding rollers, or misalignment of rollers.

To ensure smooth production, all rollers in different sections must operate at exactly the same speed; in other words, the corresponding driving gears in different stages must rotate synchronously without phase variance. In practice, however, owing to, for example, vibrations, gear damage and run-out, the rotation speed of these gears may vary. If transport speed at which axially moving web moves during manufacturing and processing reach high values, this can lead to resonance vibrations, instability or web fluttering. This behavior can result in web breaking during its motion.

To ensure that the operating system is under stable working conditions, full analysis of its dynamics has to be performed. Complete knowledge of the dynamical behavior allows the prediction and control of instabilities. Study of the transverse vibrations becomes a key to avoid possible resulting fatigue, failure, and low production quality.

1.3. Thesis Objectives

The main objectives of this thesis are the following:

1- To study free vibration of a simply supported axially moving beam following a curved path. This will be through determination of fundamental frequencies and critical speeds of the system.

2- To investigate the effect of curvature of the intermediate support on the system's response and fundamental frequency, by comparing the case of straight support without curvature.

3- To study the effect of system's parameters on the system's response. These parameters are: axial speed, applied tension, and the stiffness of the intermediate supports.

4- To study forced vibration of the axially moving beam. The system's response is studied through amplitude frequency curves, Poincare´ sections and bifurcation diagrams. We will consider the primary, sub-harmonic and super-harmonic resonances.

1.4. Thesis Overview

This thesis is organized as follows: In Chapter 2, we will present some literature on the area of axially moving materials and explain our contribution to this field. In Chapter 3, the model of the axially moving beam on a curved path used in this work will be presented in details. In Chapter 4, we include results on free vibration of the axially moving beam in terms of fundamental frequencies and critical speeds. In Chapter 5, forced vibration of the axially moving beam will be discussed. We consider cases of primary resonance, sub-harmonic and super-harmonic resonances. The results will be presented in terms of amplitude frequency curves, Poincaré sections and bifurcation diagrams of the system. In Chapter 6, we summarize our work outcomes and present some recommendations for future research.

CHAPTER 2

Literature Review

Nonlinear dynamics of axially moving materials is a very rich topic. It has been studied for over 50 years [6] due to expanding fields of application. In this chapter we will make a review of the work done in this area. Section 2.1 includes introduction of axially moving materials. Section 2.2 includes studies on axially moving beams. Section 2.3 covers studies on axially moving beams supported by elastic foundations. Section 2.4 explains the contribution of this thesis in the field.

2.1. Axially moving materials

Axially moving materials can represent many engineering devices such as power transmission belts, elevator cables, plastic films, magnetic tapes, paper sheets, textile fibers, and band saws. Any continuous and flexible material that transport axially between two rolls can be described as a web. The unwinder/winder systems handling web materials such as papers, textiles, metal strips, metal foils, plastic films, etc. are very common in the industry, because they represent a more convenient way of transporting and processing a product from one form to another. Printing, coating and drying are examples of operations that can be performed in sections of a production line. One of the main objectives in web handling machinery is to reach an expected web speed while maintaining the web stability and proper tension [7].

Despite many advantages of these devices, noise and vibrations, particularly transverse vibrations, associated with the devices have limited their applications. Therefore, understanding transverse vibrations of axially moving materials is important for the design of these devices. A good theoretical model should account for large displacements and should be capable of simulating wrinkles, which is essentially a post-buckling phenomenon.

In literature, some researchers consider a moving web as a moving string with small cross section area and a one dimension body. Other researchers prefer to model the web as a moving membrane with two dimensions. Many researchers in literature consider beam model with three dimensions. This could be the most realistic model of axially moving materials in the cases of metal sheets and conveyor belts. In this work we will consider the model of a beam to study behavior and dynamics of a moving web.

2.2. Vibrations in axially moving beams

In the early 1990s, Wickert and Mote [8] published a study on classical vibration analysis of axially moving continua. They modeled R2R webs as an axially moving strings and then as axially moving beams. They derived the equations of motion within the context of linear theory. They concluded that linear analyses cannot accurately predict the response in high speed regimes.

Wickert [9] studied the free nonlinear vibration of an axially moving elastic tensioned beam over subcritical and supercritical speed ranges. He considered transverse and longitudinal vibrations of a beam moving at a constant speed. Two coupled, nonlinear differential

equations described the beam motion along the longitudinal and transverse directions were derived using Hamilton's principle. He introduced a simplification that consisted of expressing the dynamic component of the longitudinal stress in transverse equation. He referred to results of experiments on the basis of which it was stated that longitudinal perturbations propagated much faster than the transverse ones within the technologically usable range of beam model parameters [10].

Chakraborty et al. [11] studied the non-linear modes and the associated natural frequencies of a travelling beam moving with a constant speed between two simply supported ends. They studied the hardening type nonlinearity exhibited by the system.

Öz et al. [12] investigated the response of an axially accelerating, elastic, tensioned beam. They assumed a time-dependent velocity to vary harmonically about a constant mean velocity. The influence of small fluctuations of velocity was investigated. They found that instabilities occur when the frequency of velocity fluctuations was close to two times the natural frequency of the system moving with a constant speed.

The same authors presented a study [13] on the nonlinear vibration of the beam with time dependent velocity. Based on the frequency of speed fluctuations, they studied four cases of speed variations: Zero fluctuation frequency, double the natural frequency, and near to both cases.

Pellicano and Vestroni [14] analyzed the dynamic behavior of a simply supported beam subjected to a constant axial tension and speed. The system was studied in the subcritical

and supercritical speed ranges with emphasis on the stability of the global dynamics of the system.

Chen et al. [15] considered the case of viscoelastic of beam. They investigated dynamic stability for the case of transverse parametric vibration of an axially accelerating viscoelastic tensioned beam. The material of the beam was described by the Kelvin model. The axial speed pattern was assumed as a simple harmonic variation about the constant mean speed. They presented numerical examples to demonstrate the effects of the dynamic viscosity, mean axial speed and tension on beam stability.

Ghayesh and Balar [16] studied the non-linear vibration and stability of an axially moving viscoelastic beam using the method of multiple scales. They investigated the effects of system's parameters on the time dependent amplitude, nonlinear frequency, vibrational response, frequency response, stability, and bifurcation points of the system.

Chen and Ding [17] investigated coupled vibration of an axially moving viscoelastic beam subjected to external transverse loads. Numerical results demonstrated the steady state periodic responses for transverse vibration, and starting of resonance phenomena when the external load frequency approaches one of the linear natural frequencies. The effect of material parameters and excitation parameters on the amplitude of the steady state responses were examined.

Ding and Chen [18] investigated natural frequencies of planar vibration of an axially moving beam in the supercritical speed ranges. The natural frequencies were calculated by applying Galerkin's method to the coupled longitudinal - transverse governing

equations. They presented the dependence of the first two natural frequencies on the axial speed for different flexural stiffness values.

Ghayesh [19] studied the forced vibration of an axially moving Kelvin–Voigt viscoelastic beam. Using Galerkin's approximation, he studied the response of the system in the sub critical regime, with and without internal resonance. The amplitude frequency responses and bifurcation diagrams of Poincare´ maps were presented for several values of the system's parameters.

Ding and Chen [20] investigated natural frequencies of nonlinear planar vibration of an axially moving beam numerically via Fast Fourier transform (FFT). The numerical results were compared with the first two natural frequencies of linear free transverse vibration of the beam. Results for the effect of the nonlinear coefficient on the first natural frequencies of nonlinear free transverse vibration was presented.

Huang et al. [21] analyzed the nonlinear vibration of an axially moving beam subjected to periodic force excitations. They concentrated on the stability and bifurcations of periodic solutions of the beam with internal resonance when the excitation frequency, Ω, was near the first two natural frequencies of the first and second modes of vibration and also with sub-harmonic internal resonance of a three to one ratio.

Ghayesh and Amabili [22] investigated the nonlinear forced vibration of an axially moving viscoelastic beam over the buckled state, a phenomenon occurs when the system lose its stability via a pitchfork bifurcation at a sufficiently large axial speed, known as the critical speed. They found that when the beam speed is in the supercritical regime, the system is

beyond the first instability. They examined system's responses for the cases with and without internal resonances of the beam.

Chen and Tang [23] studied the parametric stability of axially accelerating viscoelastic beam subjected to varying tension due to the axial acceleration of the beam. They discussed the assumption that, the tension is longitudinally uniform cannot be exactly held. It was an approximation that makes the governing equations mathematically easy to handle. So they investigated the parametric stability of an axially accelerating viscoelastic beam with the recognition of longitudinally varying tension.

Ghayesh et al. [24] examined the nonlinear dynamics of an axially accelerating beam in the subcritical speed regime. The analyses included the system tuned to a three to one internal resonance, as well as for the case where there was no resonance. They employed a numerical technique "the pseudo arc length continuation technique" as well as direct time integration. They also used a larger number of degrees of freedom in the Galerkin's discretization in order to analyze modal interactions.

Farokhi et al. [25] investigated the nonlinear forced dynamics of an axially moving beam numerically taking into account the in plane and out-of-plane motions. The nonlinear partial differential equations governing the motion of the system were derived via Hamilton's principle. Then, the Galerkin's scheme was introduced to these partial differential equations yielding a set of second order nonlinear ordinary differential equations with coupled terms. The bifurcation diagrams were obtained by changing either the forcing amplitude of the external excitations or the axial speed as bifurcation parameter.

Ghayesh and Amabili [26] studied the nonlinear dynamics of an axially moving beam with time dependent axial speed. They investigated the nonlinear resonant response of the system in the subcritical speed regime and global dynamical behavior. Galerkin's technique was used to discretize nonlinear partial differential equation of motion and reduced it to a set of ordinary differential equations (ODEs) by choosing the basis functions to be eigen functions of a stationary beam. Moreover, they studied the global nonlinear dynamics of the system through frequency response curves as well as bifurcation diagrams of the Poincare´ maps.

Seddighi and Eipakchi [27] studied the natural frequency and critical speed of an axially moving viscoelastic beam. The natural frequencies and the critical speed were determined by the assumption of axial speed characterized as a simple harmonic variation about a constant mean speed. By a parametric study, the effects of mechanical and geometrical parameters on the natural frequency and critical speed were investigated.

Ghayesh et al. [28] investigated the coupled nonlinear dynamics of an axially moving viscoelastic beam with time dependent axial speed. The equations of motion for both the transverse and longitudinal motions were obtained using Newton's second law of motion and the constitutive relations. A two-parameter rheological model of the Kelvin–Voigt energy dissipation mechanism was employed in the modeling of the viscoelastic beam material. Furthermore, the Galerkin's method was applied to the coupled nonlinear partial differential equation.

Yang and Zhang [29] investigated the nonlinear vibrations of an axially moving beam considering the coupling of the longitudinal and transversal motion. Their study was

conducted to determine the internal resonance in the system and its relation to axial speed and other system's parameters. They considered harmonic external excitations in both transverse and longitudinal directions.

Recently, Marynowski and Kapitaniak [30] presented a review paper on the field of axially moving materials dynamics. The paper contains a brief overview of the most important studies on the dynamics of axially moving string-like and beam-like systems. It also includes a comparative analysis of some results that have been published by other authors in the field.

Sahoo et al. [31] studied the nonlinear transverse vibration of a beam moving with a harmonically fluctuating velocity and subjected to parametric excitation at a frequency close to twice the natural frequency in the presence of internal resonance.

2.3. Axially moving beam with elastic supports

There were few researchers, who studied the case in which the beam is supported by elastic foundation. Most of them modeled the elastic foundation as a nonlinear spring placed somewhere under the moving beam.

Bağdatli et al. [32] studied the transverse vibrations of an axially accelerating beam resting on simple supports. The supports were at the two ends, and there was a support in between. The axial velocity was assumed as a sinusoidal function of time varying about a constant mean speed. Natural frequencies of the system were obtained for different locations of the third support.

16

Ghayesh [33] invisitigated the forced nonlinear vibrations of an axially moving beam additionally supported by a non-linear spring and subjected to a distributed harmonic excitation. The sub-critical response was examined when the excitation frequency was near the first natural frequency for both systems, with and without internal resonances. For different spring support coefficients, the system displayed very rich dynamical behaviour involving periodic, quasi-periodic, period-2, period-3, and chaotic motions. The author extended his work in his paper [34] to involve the effect of intermediate spring support of a viscolelastic axially moving beam.

Ghayesh et al. [35] investigated the nonlinear coupled longitudinal and transverse vibrations and stability of an axially moving beam supported by an intermediate spring. The beam was subjected to a distributed harmonic external force. Park and Chung [36] studied the transverse vibration of an axially moving finite length beam with two points were supported by rotating rollers. The rollers were modeled as uniaxial springs in the transverse direction. The variations of the natural frequencies and mode shapes are investigated for the variations of the support stiffness and position.

2.4.   Contribution

To the best of the author's knowledge, there is no published work for the effect of path curvature on the vibration of axially moving materials. Therefore, the focus of the present study is on transverse vibrations of an axially moving beam following a curved path as shown in figure 2.1.
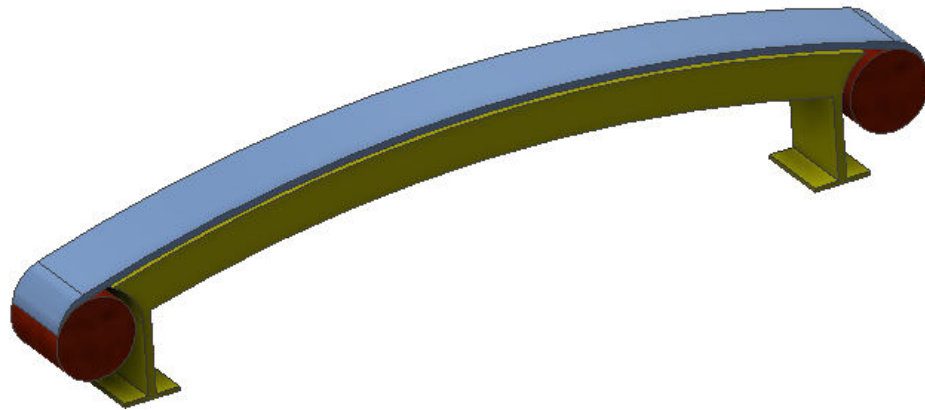
Figure 2.1 Model of the moving beam following a curved path

CHAPTER 3

Analytical Model

In this chapter, equations of motion are derived for an axially moving beam following a curved path. The Hamilton's Principle is used to derive the transverse vibration equation then, Galerkin's decomposition is applied to solve the beam equation.

3.1. Axially moving curved beam

Using a Cartesian frame of references (x-z), Figure 3.1 shows a beam traveling with an axial speed v and following a curved path. The curved path is defined by slightly curved smooth support with a combination effect of linear and nonlinear of stiffnesses k_1 and k_2. There is an axial tension P applied to the beam. The beam is subjected to an external harmonic force in the transverse direction $f = F \cos(\Omega t)$, where F is the amplitude and Ω is the frequency of excitation, t represents time coordinate.

For the axially moving beam with the characteristics presented above, the free vibration of the beam and effect of system's parameters on the fundamental frequency of the beam will be investigated. Forced vibration of the beam considering primary resonance, sub-harmonic and super-harmonic resonances, will be also studied.
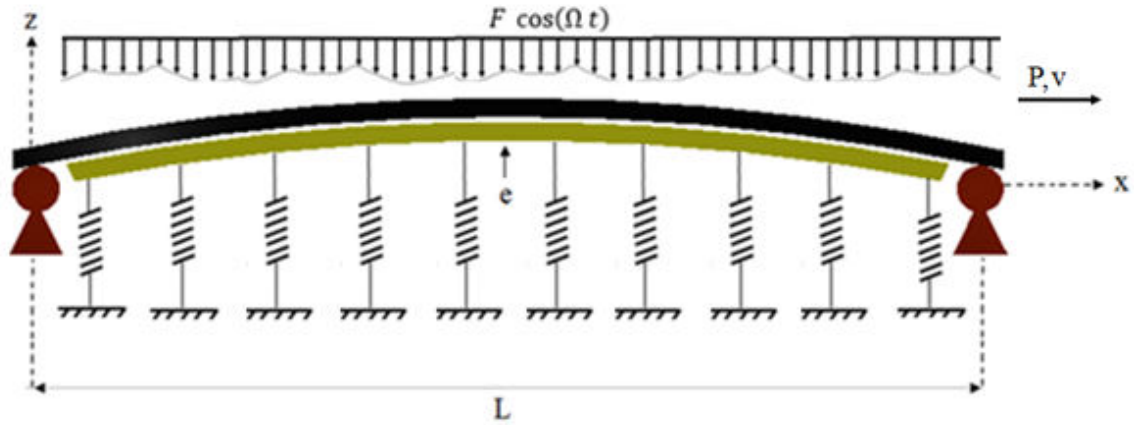
Figure 3.1 Simply supported axially moving beam following a curved path

The beam is modeled as a simply supported beam satisfying the following boundary conditions:

$$u(0,t) = u(L,t) = 0$$
(3.1)

$$w(0,t) = w(L,t) = 0, \qquad w_{xx}(0,t) = w_{xx}(L,t) = 0$$
(3.2)

Where u is axial displacement and w is transverse displacement, and the subscript x represents a derivative with respect to the x coordinate.

3.2. Strain

Let A_1 be the initial position of a point on the element at distance x in the axial direction and distance Z in the transverse direction as it is illustrated in figure 3.2. The final position of the point A_1 after deformation is A_2 with displacments x_2 and z_2.
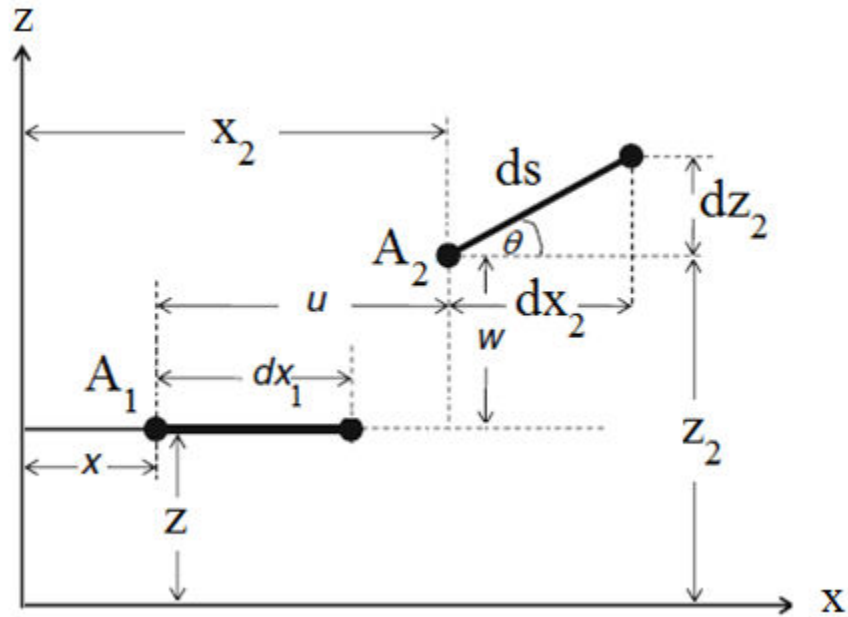
Figure 3.2 A segment of the beam with initial curvature, before and after deformation

Let us consider a differential element of length dx_1 that starts at point A_1. The point is displaced a distance u and w in the axial and transverse directions, respectively. The element length is getting deformed to ds with components dx_2 and dz_2 axially and transversely, respectively. Thus, the new coordinates of point A_2 is:

$$x_2 = x + u$$

$$z_2 = Z + w \tag{3.3}$$

Where Z represents the initial curvature of the beam caused by the curvature of the support.

Differentiating equation (3.3) with respect to x, we obtain:

$$dx_2 = \left(1 + \frac{du}{dx}\right) dx$$

$$dz_2 = \left(\frac{dZ}{dx} + \frac{dw}{dx}\right) dx \tag{3.4}$$

Therefore, after deformation we can express the length of the element, ds, as follows:

$$ds = \sqrt{(dx_2)^2 + (dz_2)^2}$$

$$ds = \sqrt{\left(1 + \frac{du}{dx}\right)^2 + \left(\frac{dz}{dx} + \frac{dw}{dx}\right)^2}\ dx \tag{3.5}$$

$$ds = \sqrt{(1 + u_x)^2 + (Z_x + w_x)^2}\ dx$$

Where the subscript notation denotes partial differentiation with respect to x.

Expanding equation (3.5) and assuming the slop of the initial rise of the curved beam to be small compared to unity (i.e., $Z_x^2 \approx 0$) [37] , we get the elongation of the differential element as

$$ds - dx = \left(\sqrt{(1 + 2u_x + u_x{}^2) + (w_x{}^2 + 2\,Z_x w_x)} - 1 \right) dx \tag{3.6}$$

Using the elongation of the deformed element, the strain of the deformed element is defined

as

$$\varepsilon = \frac{ds - dx}{dx} = \sqrt{1 + 2u_x + u_x{}^2 + w_x{}^2 + 2\,Z_x w_x} - 1 \tag{3.7}$$

Expanding equation (3.7) in a binomial series [38] yields:

$$\varepsilon = \left\{ \frac{1}{2} \left[2u_x + u_x{}^2 + w_x{}^2 + 2\,Z_x w_x \right] \right.$$
$$\left. - \frac{1}{8} \left[2u_x + u_x{}^2 + w_x{}^2 + 2\,Z_x w_x \right]^2 + \cdots \right\} \tag{3.8}$$

If one retains up to the quadratic terms in the displacement gradient u_x and w_x we obtain

the non-linear strain as

$$\varepsilon = u_x + \frac{1}{2} w_x^2 + w_x\,Z_x \tag{3.9}$$

3.3. The Kinetic Energy

The longitudinal and transverse velocity components can be derived by differentiating

equations (3.4) with respect to time:

$$\frac{dx_2}{dt} = \left(1 + \frac{du}{dx} \right) \frac{dx}{dt} + \frac{du}{dx} \frac{dx}{dt} \tag{3.10}$$

Where the longitudinal velocity $= u_t + v\,(1 + u_x)$, and

$$\frac{dz_2}{dt} = \left(\frac{dZ}{dx} + \frac{dw}{dx}\right)\frac{dx}{dt} + \left(\frac{d^2Z}{dx\,dt} + \frac{d^2w}{dx\,dt}\right)dx \qquad (3.11)$$

where the transverse velocity $= w_t + v\,(w_x + Z_x)$

The kinetic energy is then formulated as [39]:

$$T = \frac{\rho\,A}{2}\int_0^L \{[u_t + v\,(1 + u_x)]^2 + [w_t + v\,(w_x + Z_x)]^2\}\,dx \qquad (3.12)$$

Where $\rho\,A$ is the constant mass per unit length of the beam material.

3.4. The strain Energy

The strain energy of the beam due to its elastic deformation, axial tension and the energy of the linear and nonlinear supports is given by [39]:

$$U = \int_0^L \left[P\,\varepsilon + \frac{1}{2}\,E\,A\,\varepsilon^2 + \frac{1}{2}\,E\,I\,w_{xx}^2 + \frac{1}{2}k_1\,w^2 + \frac{1}{2}k_2\,w^4\right]dx \qquad (3.13)$$

3.5. Hamilton Principle Application

The Hamilton Principle states that for a particular period of time for a conservative mechanical system, the integral of the Lagrangian (difference between the Kinetic and the Potential energy) of the system is stationary [39].

$$\int_{t_1}^{t_2} (\delta T - \delta U + \delta W) \, dt = 0$$

(3.14)

where T represents kinetic energy, U represents strain energy and W is the non-conservative work exerted on the system. To apply Hamilton's Principle, Let us expand equation (3.12) for the kinetic energy:

$$T = \frac{\rho A}{2} \int_0^L \{u_t^2 + 2\,u_t\,v\,(1 + u_x) + v^2\,(1 + u_x)^2 + w_t^2 +$$

$$2\,w_t\,v\,w_x + 2\,w_t\,v\,Z_x + v^2\,w_x^2 + 2\,v^2\,w_x\,Z_x\,\} \, dx$$

(3.15)

The kinetic energy variation is obtained by integrating by parts over time all terms of equation (3.15). The detailed integrations are illustrated in the Appendix. Thus,

$$\int_{t_1}^{t_2} \delta T \, dt =$$

$$\frac{\rho A}{2} \int_{t_1}^{t_2} \left\{ \begin{array}{c} \int_0^L u_t^2 \, dx + 2\,v\,[u_t\,x]_0^L + 2\,v\,[u_t\,\delta u]_0^L - 2\,v \int_0^L u_{tx}\,\delta u\,dx \\ +v^2\,[x]_0^L + 2\,v^2[\delta u]_0^L + v^2[u_x\,\delta u]_0^L - v^2 \int_0^L u_{xx}\,\delta u\,dx \\ + \int_0^L w_t^2\,dx + 2\,v[w_t\,\delta w]_0^L - 2\,v \int_0^L w_{tx}\,\delta w\,dx \\ +v^2[w_x\,\delta w]_0^L - v^2 \int_0^L w_{xx}\,\delta w\,dx \\ +2\,v^2[Z_x\,w]_0^L - 2v^2 \int_0^L Z_{xx}\,\delta w\,dx \end{array} \right\} dt$$

(3.16)

$$\frac{\rho A}{2} \int_{t_1}^{t_2} \delta T \, dt = \int_{t_1}^{t_2} \left\{ -\int_0^L u_{tt}\,\delta u\,dx - 2\,v \int_0^L u_{tx}\,\delta u\,dx - \right.$$

$$v^2 \int_0^L u_{xx}\,\delta u\,dx - \int_0^L w_{tt}\,\delta w\,dx - 2\,v \int_0^L w_{tx}\,\delta w\,dx -$$

$$\left. v^2 \int_0^L w_{xx}\,\delta w\,dx - 2v^2 \int_0^L Z_{xx}\,\delta w\,dx \right\} dt$$

(3.17)

Now, expanding equation (3.13) to get the potential energy variation by integrating by parts over time all terms of equation (3.13). The detailed integrations are illustrated in the Appendix. The potential energy variation is given by

$$\int_{t_1}^{t_2} \delta U \, dt =$$

$$\int_{t_1}^{t_2} \left\{ \begin{array}{c} P[\delta u]_0^L + \frac{P}{2} \left[w_x \, \delta w \right]_0^L - \frac{P}{2} \int_0^L w_{xx} \, \delta w \, dx + P[\, Z_x \, \delta w \,]_0^L \\[4pt] - P \int_0^L Z_{xx} \, \delta w \, dx + \frac{EA}{2} \left[\left(u_x + \frac{1}{2} w_x^2 + w_x \, Z_x \right) \delta u \right]_0^L - \\[4pt] - \frac{EA}{2} \int_0^L \left(u_x + \frac{1}{2} w_x^2 + w_x \, Z_x \right)_x \delta u \, dx \\[4pt] + \frac{EA}{4} \left[\left(u_x + \frac{1}{2} w_x^2 + w_x \, Z_x \right) w_x \, \delta w \right]_0^L - \\[4pt] - \frac{EA}{4} \int_0^L \left[\left(u_x + \frac{1}{2} w_x^2 + w_x \, Z_x \right) w_x \right]_x \delta w \, dx \\[4pt] + \frac{EA}{2} \left[\left(u_x + \frac{1}{2} w_x^2 + w_x \, Z_x \right) Z_x \, \delta w \right]_0^L - \\[4pt] - \frac{EA}{2} \int_0^L \left[\left(u_x + \frac{1}{2} w_x^2 + w_x \, Z_x \right) Z_x \right]_x \delta w \, dx \\[4pt] + \frac{EI}{2} \left[w_{xx} \, w_x \right]_0^L - \frac{EI}{2} \left[w_{xxx} \, \delta w \right]_0^L + \\[4pt] \frac{EI}{2} \int_0^L w_{xxxx} \, \delta w \, dx + \frac{1}{2} k_1 \int_0^L w \, \delta w \, dx + \frac{1}{2} k_2 \int_0^L w^3 \, \delta w \, dx \end{array} \right\} dt \qquad (3.18)$$

$$\int_{t_1}^{t_2} \delta U \, dt = \int_{t_1}^{t_1} \left\{ -\frac{P}{2} \int_0^L w_{xx} \, \delta w \, dx - P \int_0^L Z_{xx} \, \delta w \, dx - \right.$$

$$\frac{EA}{2} \int_0^L \left(u_x + \frac{1}{2} w_x^2 + w_x \, Z_x \right)_x \delta u \, dx - \frac{EA}{4} \int_0^L \left[\left(u_x + \frac{1}{2} w_x^2 + \right. \right.$$

$$\left. w_x \, Z_x \right) w_x \right]_x \delta w \, dx - \frac{EA}{2} \int_0^L \left[\left(u_x + \frac{1}{2} w_x^2 + w_x \, Z_x \right) Z_x \right]_x \delta w \, dx + \qquad (3.19)$$

$$\left. \frac{EI}{2} \int_0^L w_{xxxx} \, \delta w \, dx + \frac{1}{2} k_1 \int_0^L w \, \delta w \, dx + \frac{1}{2} k_2 \int_0^L w^3 \, \delta w \, dx \right\} dt$$

26

The variation of non-conservative forces is given by considering the external harmonic force in the transverse direction and the viscous damping coefficient μ times the transverse speed w_t as follows:

$$\int_{t_1}^{t_2} \delta W \, dt = \int_{t_1}^{t_2} (F \, \cos(\Omega \, t) - \mu \, w_t) \, \delta w \, dt \qquad (3.20)$$

Substituting Equations (3.17), (3.19) and (3.20) in the Hamilton Principle Equation (3.14), we get

$$\frac{\rho A}{2} \int_{t_1}^{t_2} \left\{ -\int_0^L u_{tt} \, \delta u \, dx - 2v \int_0^L u_{tx} \, \delta u \, dx - v^2 \int_0^L u_{xx} \, \delta u \, dx - \right.$$

$$\int_0^L w_{tt} \, \delta w \, dx - 2v \int_0^L w_{tx} \, \delta w \, dx - v^2 \int_0^L w_{xx} \, \delta w \, dx -$$

$$\left. 2v^2 \int_0^L Z_{xx} \, \delta w \, dx \right\} dt - \int_{t_1}^{t_2} \left\{ -\frac{P}{2} \int_0^L w_{xx} \, \delta w \, dx - P \int_0^L Z_{xx} \, \delta w \, dx - \right.$$

$$\frac{EA}{2} \int_0^L \left(u_x + \frac{1}{2} w_x^2 + w_x Z_x \right)_x \delta u \, dx - \frac{EA}{4} \int_0^L \left[\left(u_x + \frac{1}{2} w_x^2 + \right. \right.$$

$$\left. w_x Z_x \right) w_x \right]_x \delta w \, dx - \frac{EA}{2} \int_0^L \left[\left(u_x + \frac{1}{2} w_x^2 + w_x Z_x \right) Z_x \right]_x \delta w \, dx +$$

$$\left. \frac{EI}{2} \int_0^L w_{xxxx} \, \delta w \, dx + \frac{1}{2} k_1 \int_0^L w \, \delta w \, dx + \frac{1}{2} k_2 \int_0^L w^3 \, \delta w \, dx \right\} dt +$$

$$F \, \cos(\Omega \, t) - \int_{t_1}^{t_2} \mu \, w_t \, \delta w \, dt = 0$$

(3.21)

Because Equation (3.21) must hold for any arbitrary δu, δw and δu_x, δw_x, the integrand part must be zero, which gives the governing equations of motion for transverse and longitudinal vibrations of the beam. Gathering the terms with coefficient "δu" and multiplying by -2, we obtain

$$\rho \, A \, u_{tt} + 2 \, \rho \, A \, v \, u_{tx} + \rho \, A \, v^2 \, u_{xx} - EA \left(u_x + \frac{1}{2} w_x^2 + w_x \, Z_x \right)_x = 0 \qquad (3.22)$$

Also, gathering the terms with coefficient "δw" and multiplying by -2, we obtain

$$\rho \, A \, w_{tt} + 2 \, v \, \rho \, A \, w_{tx} + v^2 \, \rho \, A \, w_{xx} + 2 \, v^2 Z_{xx} - P \, w_{xx} - 2 \, P \, Z_{xx} +$$

$$2 \, \mu \, w_t + EI \, w_{xxxx} + k_1 \, w + k_2 \, w^3 - \frac{EA}{2} \left[\left(u_x + \frac{1}{2} w_x^2 + w_x \, Z_x \right) w_x \right]_x -$$

$$EA \left[\left(u_x + \frac{1}{2} w_x^2 + w_x \, Z_x \right) Z_x \right]_x = 2 \, F \, \cos(\Omega \, t) \qquad (3.23)$$

Equations (3.22) and (3.23) represent, respectively, the longitudinal and transverse governing equations describing vibration of the beam. In order to solve these equations, we introduce the following non-dimensional parameters for normalization:

$$u^* = \frac{u}{L} \qquad w^* = \frac{w}{L} \qquad Z^* = \frac{Z}{L} \qquad x^* = \frac{x}{L} \qquad t^* = \frac{t}{T} \qquad (3.24)$$

Substituting expressions in (3.24) into Equations (3.22) and (3.23) and multiplying by L/P yields

$$\frac{\rho \, A \, L^2}{P \, T^2} \frac{\partial^2 u^*}{\partial t^{*2}} + 2 \, \frac{\rho \, A \, v \, L}{P \, T} \frac{\partial^2 u^*}{\partial t^* \, \partial x^*} + \frac{\rho \, A \, v^2}{P} \frac{\partial^2 u^*}{\partial x^{*2}} - \frac{EA}{P} \frac{d}{dx^*} \left\{ \frac{\partial u^*}{\partial x^*} + \right.$$

$$\left. \frac{1}{2} \left(\frac{\partial w^*}{\partial x^*} \right)^2 + \frac{\partial w^*}{\partial x^*} \frac{\partial Z^*}{\partial x^*} \right\} = 0 \qquad (3.25)$$

and

28

$$\frac{\rho\,A\,L^2}{P\,T^2}\frac{\partial^2 w^*}{\partial t^{*2}} + 2\,\frac{\rho\,A\,v\,L}{P\,T}\frac{\partial^2 w^*}{\partial t^*\,\partial x^*} + \frac{\rho\,A\,v^2}{P}\frac{\partial^2 w^*}{\partial x^{*2}} + 2\,\frac{\rho\,A\,v^2}{P}\frac{\partial^2 Z^*}{\partial x^{*2}} -$$

$$\frac{\partial^2 w^*}{\partial x^{*2}} - 2\,\frac{\partial^2 Z^*}{\partial x^{*2}} + 2\,\frac{\mu\,L^2}{P\,T}\frac{\partial w^*}{\partial t^*} + \frac{EI}{PL^2}\frac{\partial^4 w^*}{\partial x^{*4}} + k_1\frac{L^2}{P}\,w^* +$$

$$k_2\frac{L^4}{P}\,{w^*}^3 - \frac{EA}{2\,P}\frac{d}{dx^*}\left\{\left(\frac{\partial u^*}{\partial x^*} + \frac{1}{2}\left(\frac{\partial w^*}{\partial x^*}\right)^2 + \frac{\partial w^*}{\partial x^*}\frac{\partial Z^*}{\partial x^*}\right)\frac{\partial w^*}{\partial x^*}\right\} - \tag{3.26}$$

$$\frac{EA}{P}\frac{d}{dx^*}\left\{\left(\frac{\partial u^*}{\partial x^*} + \frac{1}{2}\left(\frac{\partial w^*}{\partial x^*}\right)^2 + \frac{\partial w^*}{\partial x^*}\frac{\partial Z^*}{\partial x^*}\right)\frac{\partial Z^*}{\partial x^*}\right\} = \frac{2\,F\,L}{P}\cos(\Omega\,T\,t^*)$$

Using the non-dimensional parameters defined in table (3.1), simplifying equations (3.25)

and (3.26) and dropping the asterisk notations for brevity give

$$u_{tt} + 2\,c\,u_{tx} + c^2\,u_{xx} - v_1{}^2\frac{d}{dx}\left\{u_x + \frac{1}{2}w_x^2 + w_x\,Z_x\right\} = 0 \tag{3.27}$$

$$w_{tt} + 2\,c\,w_{tx} + (c^2 - 1)\,w_{xx} + 2\,(c^2 - 1)Z_{xx} + 2\,\mu\,w_t +$$

$$v_f{}^2\,w_{xxxx} + \alpha_1\,w + \alpha_2\,w^3 - \frac{1}{2}v_1{}^2\frac{d}{dx}\left\{\left(u_x + \frac{1}{2}w_x^2 +\right.\right.$$

$$\left.\left. w_x\,Z_x\right)w_x\right\} - v_1{}^2\frac{d}{dx}\left\{\left(u_x + \frac{1}{2}w_x^2 + w_x\,Z_x\right)Z_x\right\} = G\cos(\Omega\,t) \tag{3.28}$$

29

Table 3.1 The Non-dimensional parameters

Parameter	Definition
$c = v\sqrt{\dfrac{\rho A}{P}}$	The transport speed parameter
$v_1 = \sqrt{\dfrac{EA}{P}}$	The longitudinal stiffness parameter
$v_f = \sqrt{\dfrac{EI}{PL^2}}$	The flexural stiffness parameter
$T = t\sqrt{\dfrac{\rho A L^2}{P}}$	Time dimensionless parameter
$\alpha_1 = \dfrac{k_1 L^2}{P}$	The linear coefficient of the curved foundation
$\alpha_2 = \dfrac{k_2 L^4}{P}$	The nonlinear coefficient of the curved foundation
$\mu^* = \dfrac{\mu L^2}{PT}$	The damping parameter
$G = \dfrac{2 F L}{P}$	External force amplitude
$\Omega^* = \Omega T$	External force frequency

We can suppress the appearance of u in the transverse vibration equation (3.28) using the approximation given in [9]. It is assumed that the influence of longitudinal inertia is small, then, equation (3.27) is given by:

$$\left(u_x + \frac{1}{2} w_x^2 + w_x\, Z_x \right)_x = 0 \tag{3.29}$$

and the axial strain is approximated to:

$$\frac{\partial u_x}{\partial x} = \varepsilon_x = \int_0^L \left(\frac{1}{2} w_x^2 + w_x\, Z_x \right) dx \tag{3.30}$$

Substituting equations (3.29) and (3.30) into equation (3.28) we get:

$$w_{tt} + 2\,c\,w_{tx} + (c^2 - 1)\,w_{xx} + 2\,(c^2 - 1)\,Z_{xx} + 2\,\mu\,w_t + \\ 2\,v_f{}^2\,w_{xxxx} + \alpha_1\,w + \alpha_2\,w^3 - \frac{1}{2} v_1{}^2 (w_{xx} + 2\,Z_{xx}) \int_0^1 \left(\frac{1}{2} w_x^2 + \\ w_x\, Z_x \right) dx = G \cos(\Omega\,t\,) \tag{3.31}$$

3.6.   Galerkin's method

In order to solve equation (3.31), the Galerkin's method is applied to the equation of motion to discretize it into a set of nonlinear ordinary differential equations. Hence, the eigen functions of a simply supported beam are chosen as the basis functions for the following separation of variables technique:

$$w(x,t) = \emptyset(x)\, q(t)$$

(3.32)

where $\emptyset(x)$ is the mode shape of the transverse motion of a simply supported beam given by equation (3.33)

$$\emptyset(x) = \sin\left(\frac{i\,\pi x}{L}\right)$$

(3.33)

where i is the number of vibration mode, and $q(t)$ represents the time function for the transverse direction.

The curvature Z of the path followed by the beam is assumed to have a half-sine wave Accordingly, the formula that describes the curvature shape is:

$$Z(x) = e\,\sin\left(\frac{\pi x}{L}\right)$$

(3.34)

with an amplitude e at the center to describe the degree of curvature, i.e. if e is zero, then we deal with a straight beam, if e is greater than one then the beam has a curved shape which is upward curvature (as seen in figure 3.3).
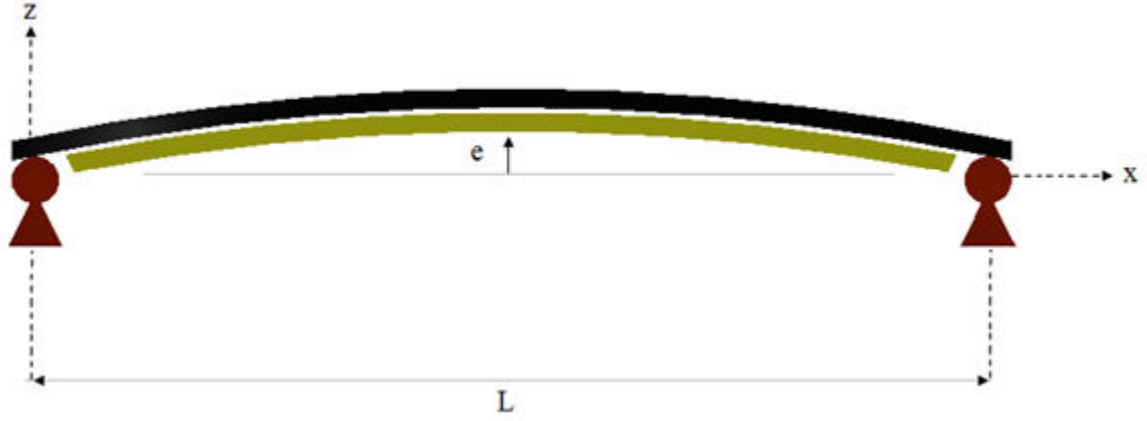
Figure 3.3 Curved path configuration with curvature amplitude ' e '

Our assumption for the curvature function goes along with literature in this topic. The idea of curvature in literature is studied for stationary beams only by few researchers [40]–[43]. In all of these papers, a sinusoidal curvature function was assumed.

Substitute equations (3.33) and (3.34) and their derivatives into equation (3.31), we get the transverse vibration equation as:

$$
\begin{aligned}
&\alpha_2 \sin^3(\pi x)\, q^3 + \Big[\alpha_1 + \pi^2(1 - c^2) + \pi^4\, v_f^2 + \\
&\frac{1}{8}\, \pi^4\, q^2\, v_1^2 \Big] q\, \sin(\pi x) + 2\,\pi\, c\, \cos(\pi x)\, \dot{q} + \sin(\pi x) \Big[2\, \pi^2\, e\, (1 - \\
&c^2) + \frac{1}{2}\, \pi^4\, e^2\, q\, v_1^2 + \frac{1}{2}\, \pi^4\, e\, q^2\, v_1^2 + 2\, \mu\, \dot{q} + \ddot{q}\Big] = 0
\end{aligned}
\tag{3.35}
$$

Multiplying the resulting equation by the first mode shape $sin(\pi x)$, then integrating with respect to x over the domain from 0 to 1, and multiplying by 2, the transverse vibration equation is simplified into

33

$$\ddot{q} + 2\,\mu\,\dot{q} + \left[\alpha_1 + \pi^2(1-c^2) + \pi^4\,v_f{}^2 + \frac{1}{4}\,\pi^4\,e^2\,v_1{}^2\right]q +$$
$$\left[\frac{1}{2}\,\pi^4 e\,v_1{}^2\right]q^2 + \left[\frac{3}{32}\,\pi^4\,v_1{}^2 + \frac{3}{4}\,\alpha_2\right]q^3 + 2\,\pi^2(1-c^2)\,e = 0 \qquad (3.36)$$

Finally, we get the final form of the equation describing free transverse vibration in time coordinate as:

$$\ddot{q} + 2\,\mu\,\dot{q} + a\,q + bq^2 + d\,q^3 + 2\,\pi^2\,(1-c^2)\,e = 0 \qquad (3.37)$$

Where:

$$a = \omega^2 = \left[\alpha_1 + \pi^2(1-c^2) + \pi^4\,v_f{}^2 + \frac{1}{4}\,\pi^4\,e^2\,v_1{}^2\right] \qquad (3.38)$$

$$b = \left[\frac{1}{2}\,\pi^4\,e\,v_1{}^2\right] \qquad (3.39)$$

$$d = \left[\frac{3}{32}\,\pi^4\,v_1{}^2 + \frac{3}{4}\,\alpha_2\right] \qquad (3.40)$$

Equation (3.38) represents a second-order inhomogeneous nonlinear differential equation, which has both quadratic and cubic nonlinearity. The first coefficient a represents the squared first "fundamental" natural frequency of beam vibration in transverse direction. The second coefficient b is responsible of the quadratic nonlinearity in the equation due the curvature e. The third coefficient d represent the cubic nonlinearity comes from mid-plan stretching of the beam about its neutral axis while it vibrates and from the nonlinear elastic foundation parameter k_2.

CHAPTER 4

Free vibration of axially moving beam moving in a

curved path

For studying the free vibration case, let us consider a simply supported axially moving beam following a curved path. Let us consider a steel beam with the properties shown in Table 4.1.

Table 4.1 System parameters

Parameter	Definition
$L = 1\ m$	Length of the beam
$b = 4\ cm$	Width of the beam
$h = 4\ mm$	Thickness of the beam
$\rho = 7.8 * 10^3\ kg/m^3$	Density of the beam material
$E = 2.1 * 10^{11}\ N/m^2$	Modulus of elasticity of the beam
$k_1 = 800\ N/m$	The linear stiffness of the foundations
$k_2 = 8000\ N/m$	The nonlinear stiffness of the foundations

The curved path has an amplitude ranges from $1\ to\ 2\ cm$ at the middle of the beam. The path is supported by an elastic foundation with a combination of linear and nonlinear stiffnesses. The beam travels axially with a speed $v = 1m/s$ and subjected to an axial tension $P = 100\ N$.

This chapter include a discussion on the free vibration of the beam. In sections 4.1 to 4.6 we consider the first mode of vibration and discuss system nonlinearities, natural frequency, critical speed, wave form, and phase portrait for transverse vibration of the beam.

4.1.   System Nonlinearities

Nonlinear systems are characterized by the fact that the superposition principle does not apply. In general, nonlinearities in structural mechanics arise in many different ways and take different forms including material, geometric, inertial, and frictional nonlinearities.

Material nonlinearities exist in systems which exhibit nonlinear stress - strain relationships, such as the elastic - plastic behavior. Geometric nonlinearities arise from nonlinear strain - displacement relationships. Sources of this type of nonlinearity include mid-plane stretching, large curvatures of structural elements, and large rotation of elements. Inertia nonlinearities arise as a result of concentrated or distributed masses. Friction nonlinearities, arise, for example, from dry friction, stick slip, and hysteresis [44].

The governing equation of the axially moving beam, equation 3.37 includes two nonlinear terms associated with the quadratic and cubic terms. The first one is due to the curvature

of the path of the axially moving beam, while the second one is due to the tension or stretching of the beam's neutral axis during vibration in addition to the nonlinear elastic foundation parameter.

The coefficients of the nonlinear terms are functions of many parameters. Figure 4.1 shows the effect of path of axial motion curvature on the coefficient of quadratic nonlinearity. By increasing the curvature of the beam the coefficient of quadratic nonlinearity increases linearly.
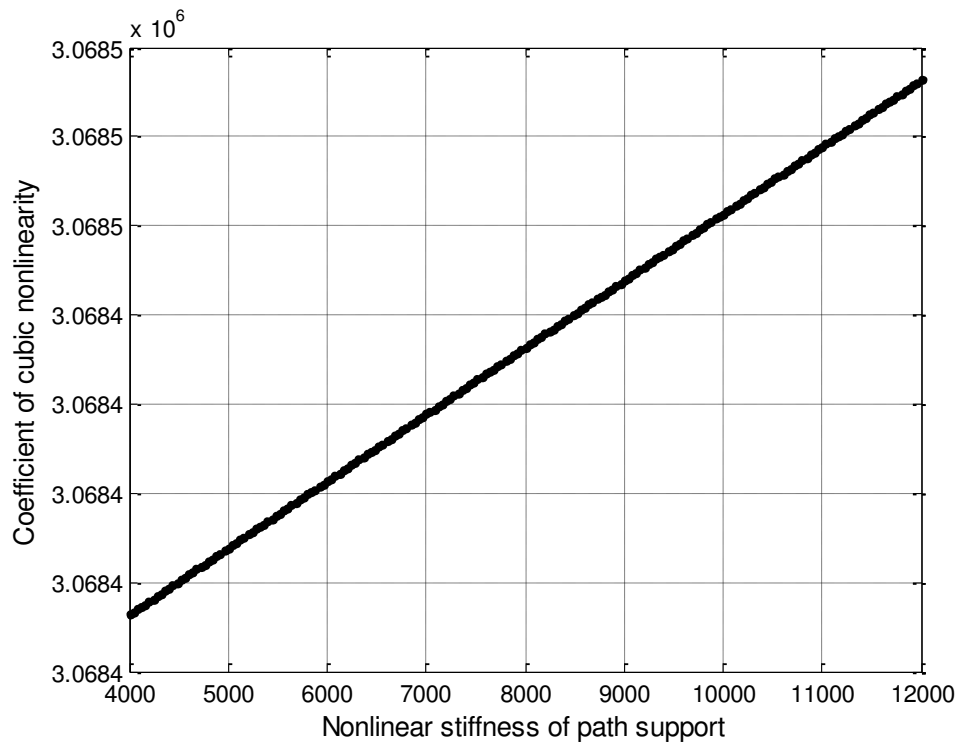
Figure 4.2 shows the effect of nonlinear stiffness of the path supports in the coefficient of cubic nonlinearity. By increasing the stiffness of the supports the coefficient of cubic nonlinearity increases linearly.

From figures 4.1 and 4.2 we can see the nonlinear terms coefficients are relatively high, with power 10^5 which produce stiff second ordinary differential equation. An ordinary differential equation problem is stiff if the solution varies slowly, but there are nearby solutions that vary rapidly, so small steps must be used carefully to obtain satisfactory numerical solution.

To get an accurate solution we increased the simulation time to 1430 seconds and reduced the time intervals to 0.007 of a second. We used absolute and relative tolerances equals 10^{-6} to guarantee more accuracy. Relative tolerance is a measure of the error relative to the size of each solution component. Roughly, it controls the number of correct digits in all solution components, except those that are smaller than thresholds of absolute tolerance.
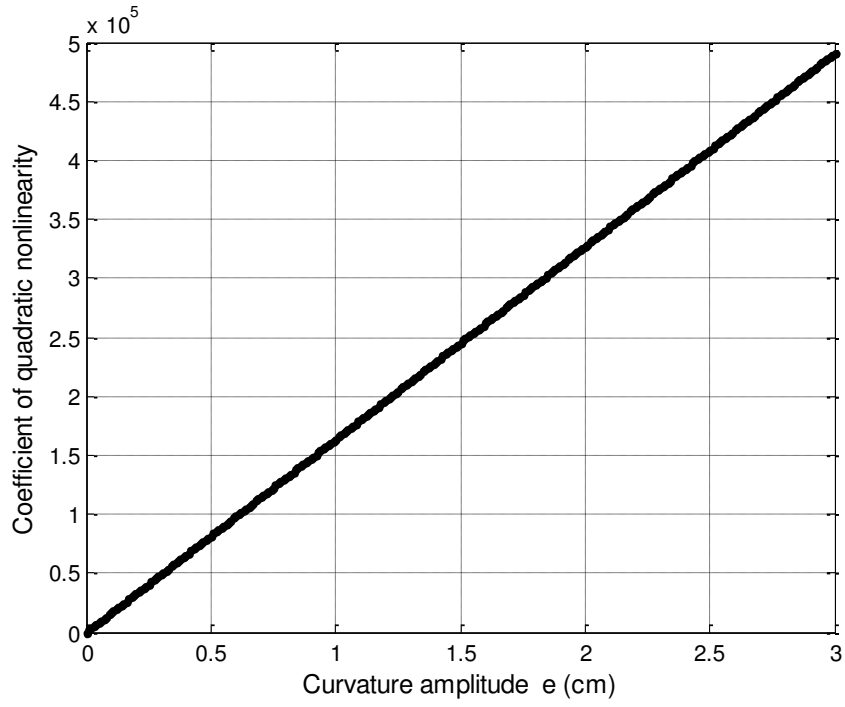
Figure 4.1 Coefficient of quadratic nonlinearity versus curvature amplitude


Figure 4.2 Coefficient of cubic nonlinearity versus nonlinear stiffness of the support at curvature amplitude e=2 cm

4.2. Natural frequency

In this section, the combined effects of geometrical and other parameters including axial tension, axial velocity and support stiffnesses on the natural frequency of an axially moving beam on a curved elastic support are investigated.

The fundamental frequency is given by equation (3.39). Figure 4.3 shows the effect of curvature amplitude e on the fundamental natural frequency. The natural frequency increases with increasing the amplitude of beam curvature. We can compare the natural frequency of a straight beam with the case when the beam is supported by a curved path for different values of curvature. We realize that the natural frequency is much higher for the beam following a curved path. This is due to the fact that the natural frequency equation contains a term of amplitude of curvature multiplied by flexural stiffness parameter multiplied by π^4 which causes higher frequencies. These products magnify the natural frequency.
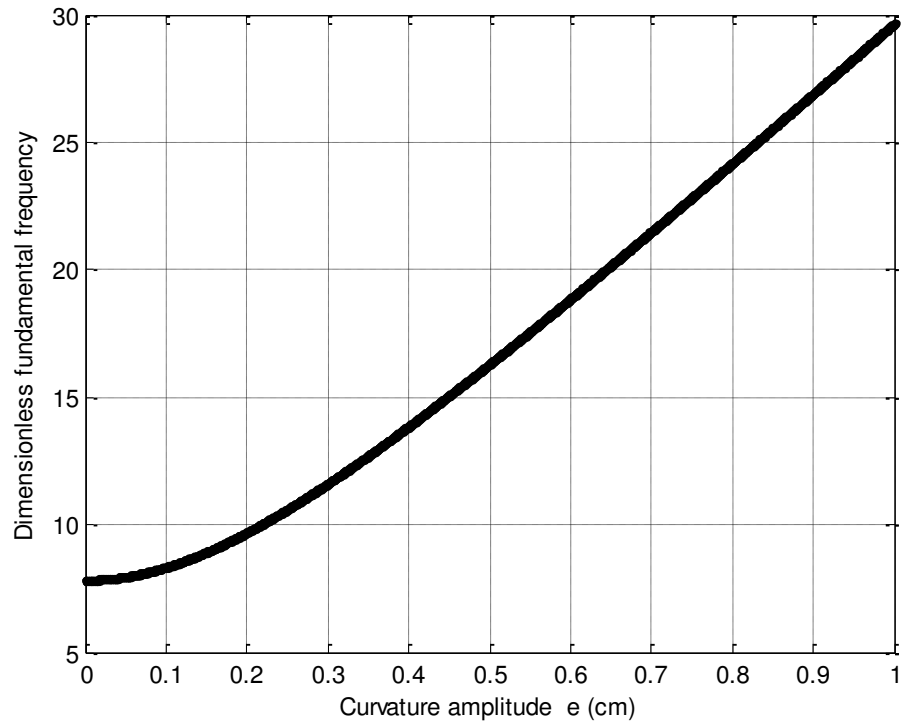
Figure 4.3 Frequency versus path curvature amplitude 'e '

Figure 4.4 shows the effect of curvature on the natural frequency for different values of axial tension of the beam, P. It is clearly seen that the curvature produces a significant increase in the natural frequency when higher tension is applied. While in case of straight beam where $e = 0$ the increase in axial tension slightly affect the fundamental frequency.
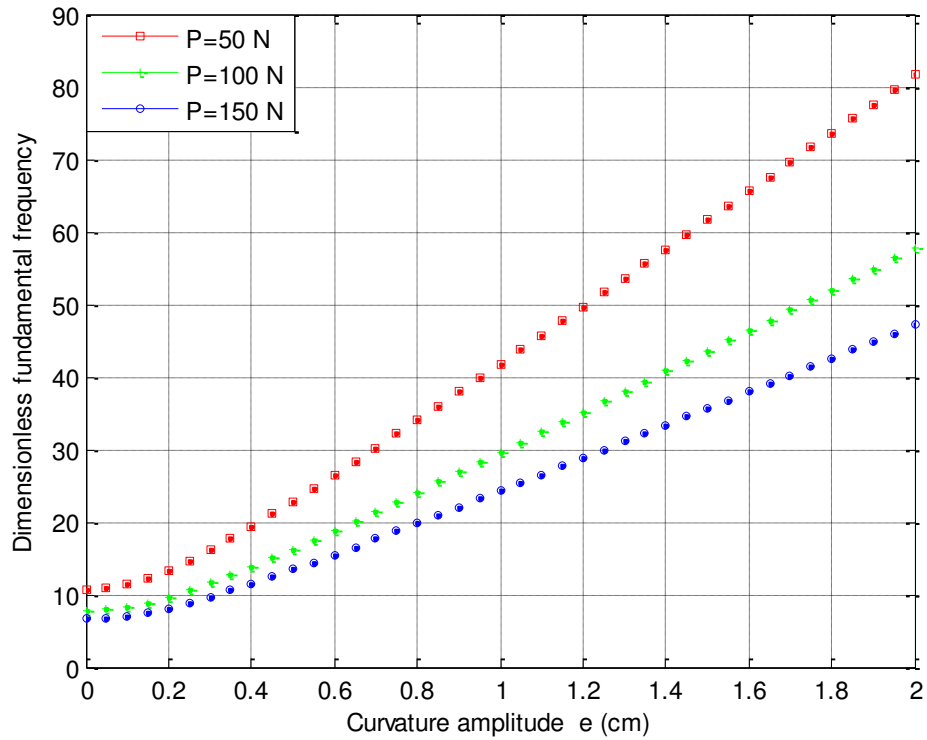
Figure 4.4 Frequency versus path curvature amplitude for different values of axial tension

Figure 4.5 shows the effect of curvature on the natural frequency for different values of axial speed. As the amplitude of path curvature increases the effect of axial speed on natural frequency is reduced.

Figure 4.6 shows the effect of applied axial tension, P on the fundamental frequency for different values of speed. It is clear that increasing axial tension decreases the natural frequency. The figure is plotted when curvature $e = 1\ mm$. While for higher values of curvature amplitude, changing axial speed does not make notable difference.
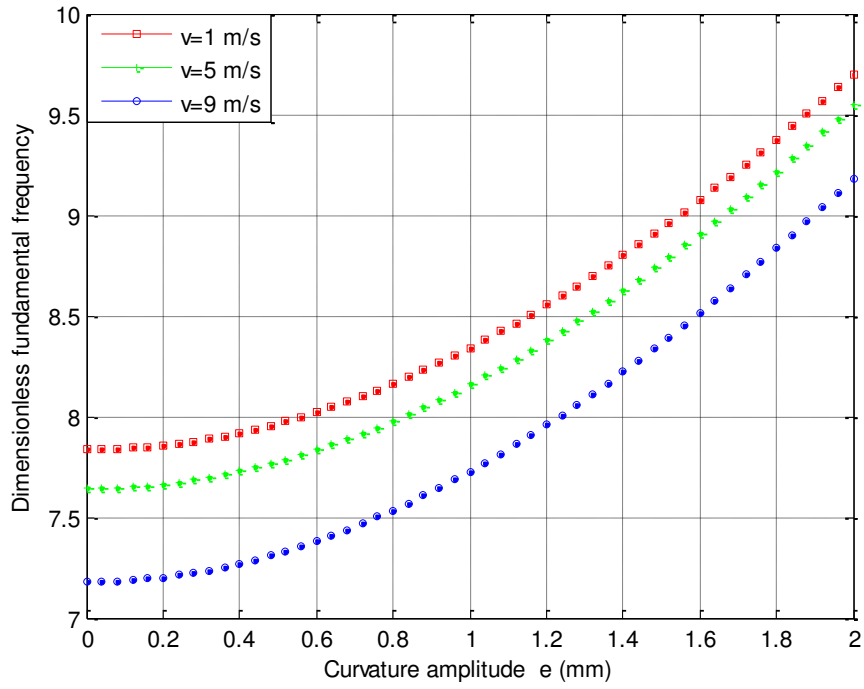
Figure 4.5 Frequency versus path curvature amplitude for different values of axial speed
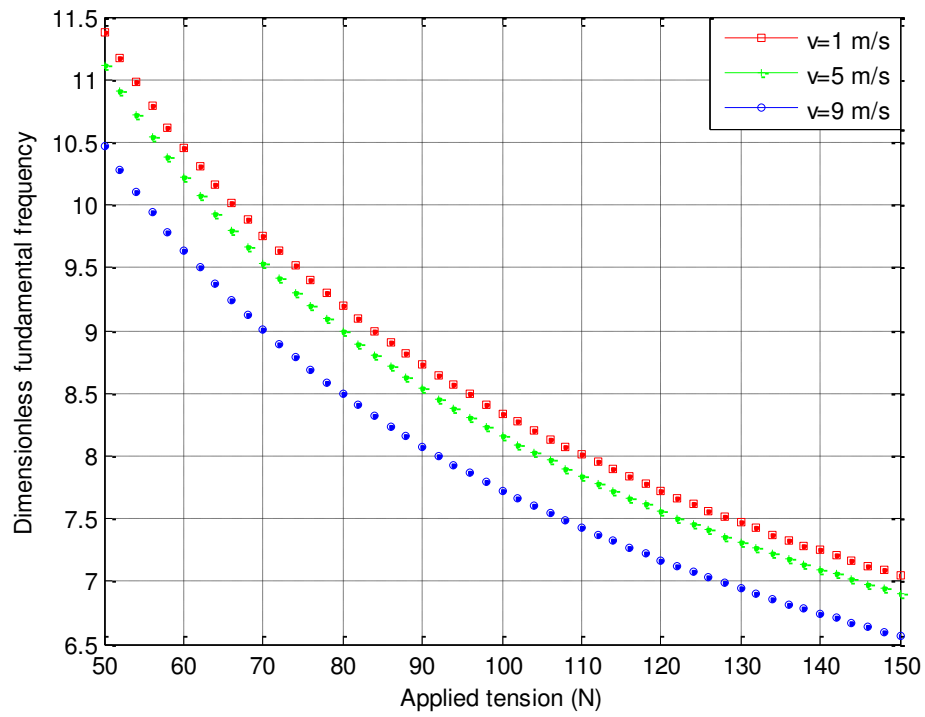
Figure 4.6 Frequency versus axial tension for different values of speed $e = 1\ mm\ k_1 = 800\ N/m$

42

Figure 4.7 shows the effect of applied axial tension, P, on the natural frequency for different values of stiffness of the path supports. The variation in frequency caused by changing stiffness is small compared to the main system parameters [axial speed and axial tension]. We realize that the figure is plotted when curvature $e = 1\ mm$, and for higher values of curvature the effect of changing stiffness of the supports is very small.
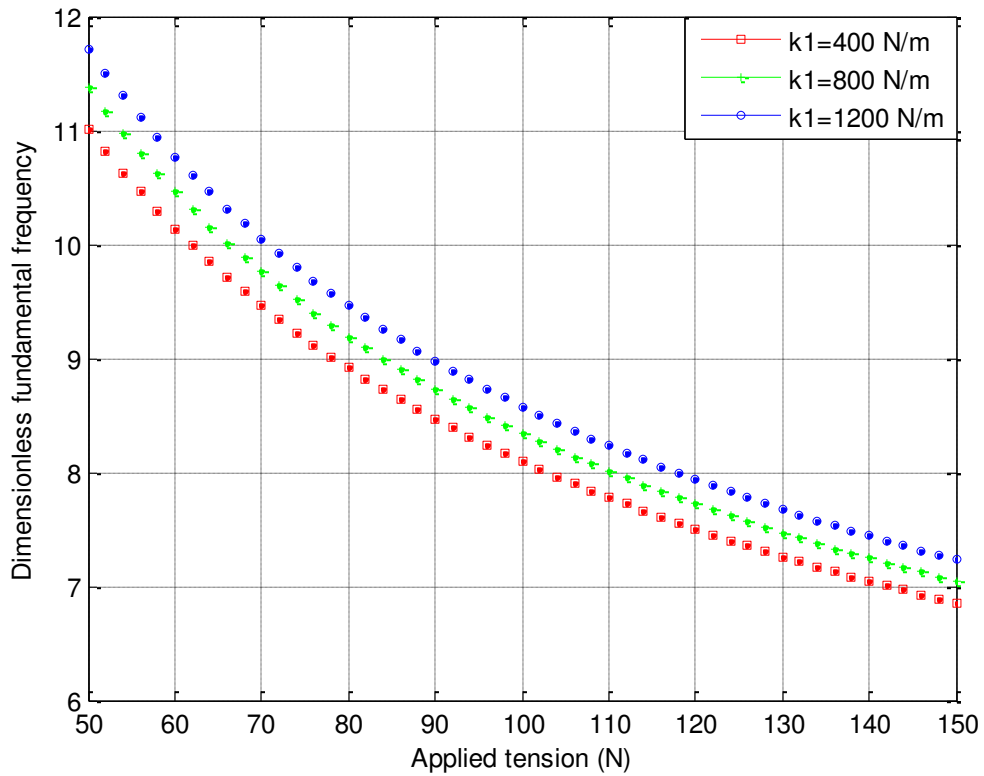
Figure 4.7 Frequency versus tension for different values of stiffness of path supports at curvature amplitude
$e = 1\ mm$

4.3. Critical speed

The critical speed of a moving beam is the value that makes the fundamental frequency vanish [45]. It corresponds to the equilibrium solution for equation (3.31).If we set equation (3.39) to zero, we get an expression for the critical speed C^*

$$C^* = \sqrt{\left[\frac{\alpha_1}{\pi^2} + 1 + \pi^2 v_f{}^2 + \frac{1}{4} \pi^2 e^2 v_1{}^2\right]} \qquad (4.1)$$

Figure 4.8 shows the variation of critical speed with fundamental frequency for an axially moving beam with e=1 mm, P=100 N, $k_1 = 800\ N/m$ the natural frequency vanishes at dimensionless speed of 2.8 which is equivalent to 25 m/s.
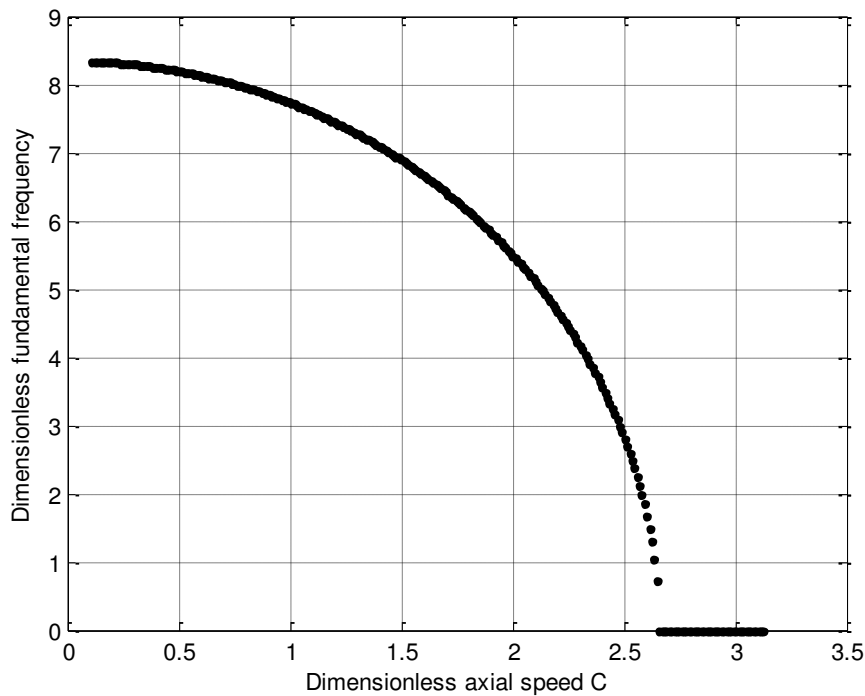
Figure 4.8 Fundamental frequency versus axial speed; at curvature amplitude e=1 mm, P=100 N, $k_1 = 800\ N/m$

44

Figure 4.9 shows the relationship between critical speed and amplitude of path curvature. If we compare the case when, $P = 100\ N$, the dimensionless critical speed of a straight beam will be 2.5 equivalent to $(20.6\ m/s)$ while the same beam supported by a curved path with an amplitude $e = 2\ mm$ with stiffness of the supporting path $k_1 = 800\ N/m$ and $k_2 = 8000\ N/m$ will increase the dimensionless critical speed to be 3.6 equivalent to $(32.2\ m/s)$. These are a high values compared to normal working speed in R2R systems for material handling in general [46] which is about 2.5 m/s, or specifically less than 10 m/s for newspaper printing [5].
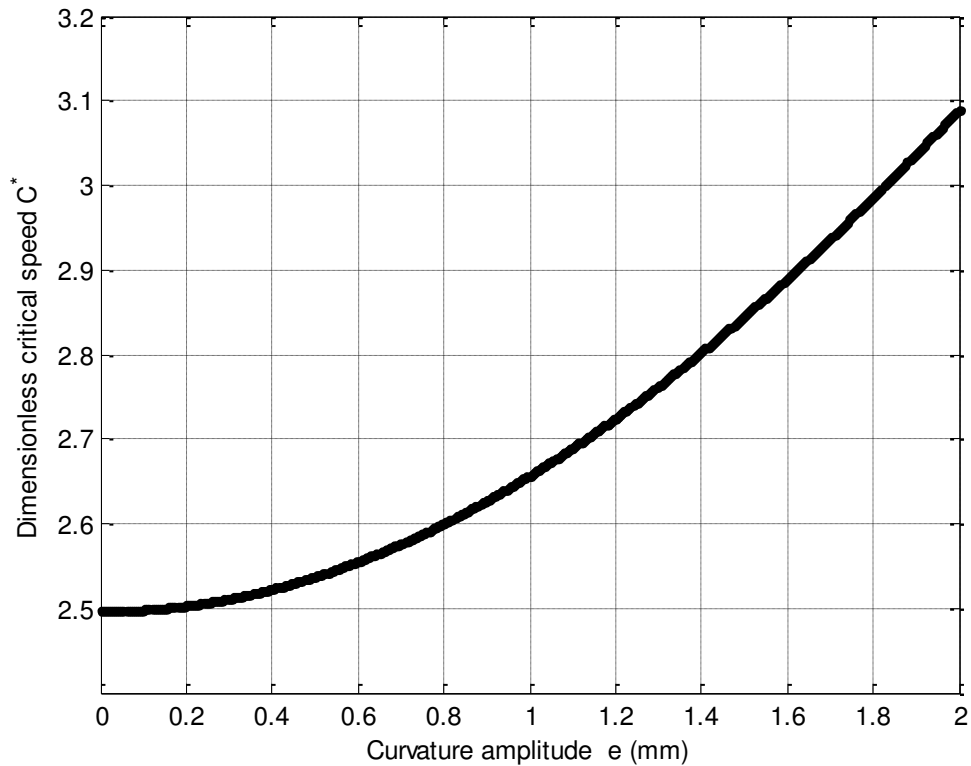
Figure 4.9 Critical speed versus curvature amplitude of the path; at P=100 N, $k_1 = 800\ N/m$

To show the effect of curvature on the critical speed, we plot the relationship between fundamental frequency and dimensionless speed for different values of curvature amplitude as shown in figure 4.10. We note that higher values of curvature amplitudes corresponds to higher values of critical speeds.
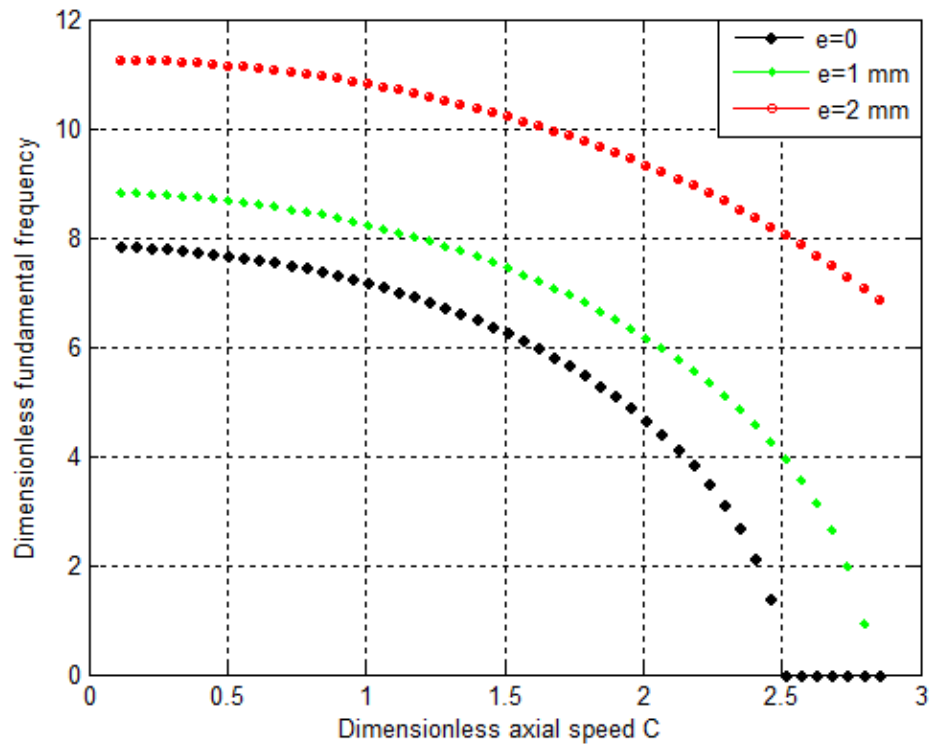
Figure 4.10 Natural frequency versus axial speed, at P=100 N, $k_1 = 800\ N/m$ for different values of curvature amplitudes

Figure 4.11 shows the relation between dimensionless critical speed and applied axial tension. The critical speed decreases as axial tension increases.

Figure 4.11 Critical speed versus applied tension; at e=1 mm, $k_1 = 800\ N/m$

4.4.   Waveform and Phase portrait

Waveforms and phase portraits can be observed to discern chaotic behaviors from regular behaviors of dynamical systems. In this section, we plot the waveform and the phase portrait for free vibration of an axially moving beam in transverse direction. We use a beam with the parameters given in table 4.1.

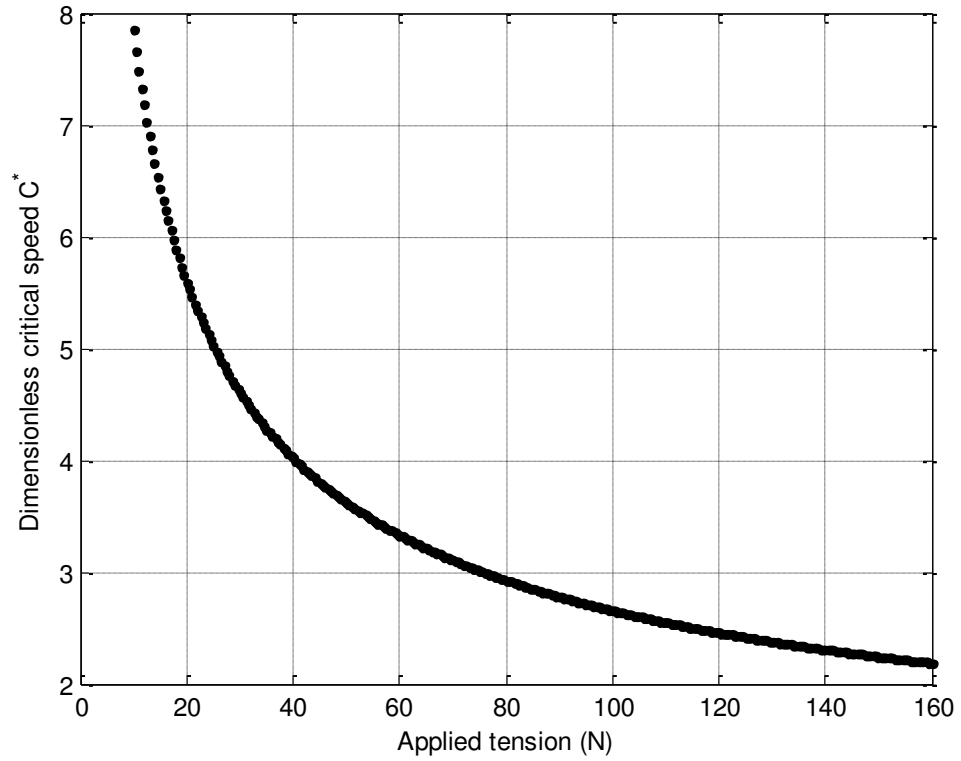Generally, visualization of time waveforms is a straightforward method for dynamic system analysis because periodic waveforms represent a pattern. Chaotic waveforms appear to be shaking. In other words, Waveforms of equilibrium or periodic behaviors are regular while the waveform of a chaotic behavior is irregular.

The phase portrait is the geometric representation of the system trajectories in the phase plane, and involves coordinate frames defined by the independent variables that describe the system dynamics where all possible states can be represented. Showing phase portraits are an important tool for the study of dynamic systems, and reveal information such as whether an attractor, or a limit cycle is present for a chosen parameter values. While a stationary system is represented by a fixed point in the phase plane, a periodic system presents a closed orbit (limit cycle). A chaotic behavior is characterized by irregular trajectories confined to a well-defined region in the phase plane, known as stranger attractor, where orbits never repeat the same trajectory.

4.4.1. Effect of path curvature

To investigate the effect of the curved elastic support on the vibration of an axially moving beam, let us first show system's response for the case of a straight elastic support with zero amplitude of curvature. Figure 4.12 shows the waveform and phase portrait for a straight axially moving vibrating beam. Assuming initial conditions as $q_0 = 1\ cm$, $\dot{q}_0 = 0$, we realize that the response does not exceed the initial displacement. The wave form and the phase portrait show a typical characteristics of a periodic motion where the beam oscillates between negative and positive $1\ cm$ from the horizontal datum.
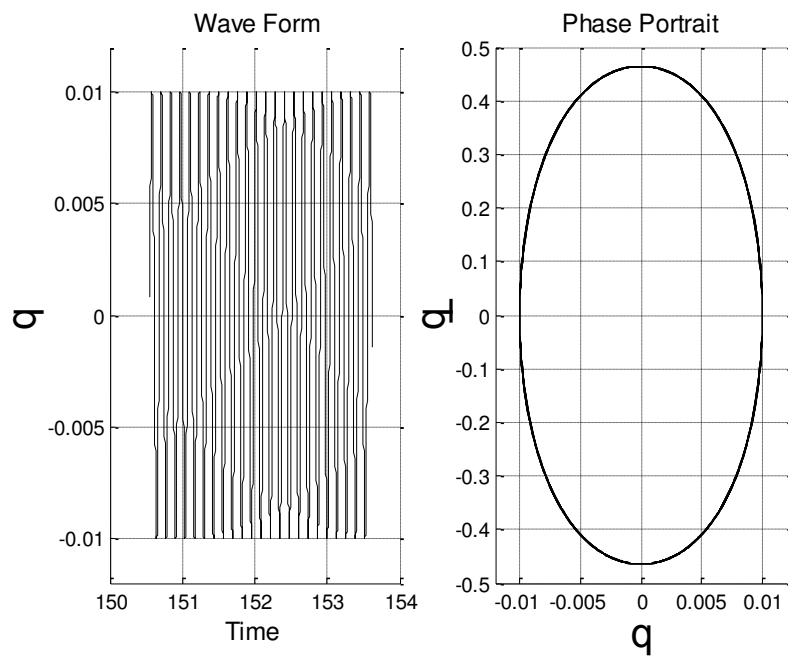
Figure 4.12 Time history and phase portrait for transverse vibration at e= 0

In figure 4.13 we impose an amplitude of path curvature of 1 cm. One can see the downward shift in the response to give higher values in the negative direction. The effect of path curvature is also clear in phase portrait as an in-periodicity in system's response.
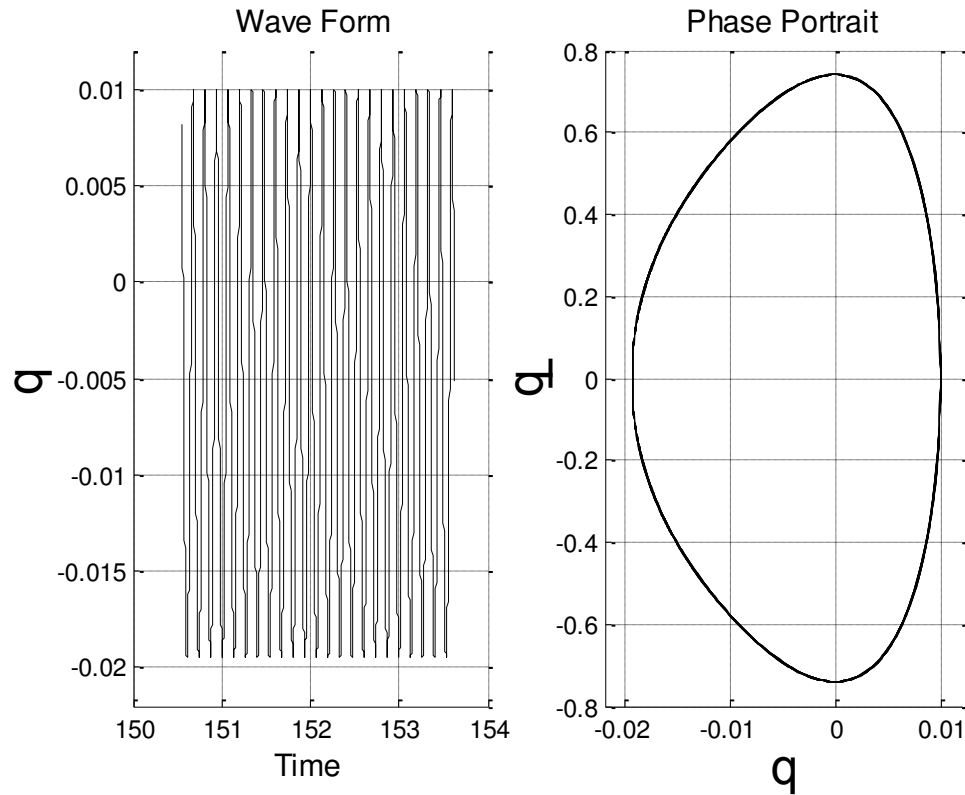
Figure 4.13 Time history and phase portrait for transverse vibration at e= 1 cm , k₁=1.5*10^5 , k₂=10 k₁

4.4.2. Effect of stiffness of the support

We simulate the system many times with different values of support stiffness. For a beam with a curvature amplitude $e = 2$ cm and values of stiffness $k_1 = 8 * 10^5 \ N/m$ and $k_2 = 80 * 10^5 \ N/m$ the beam vibration has small in-periodicity with maximum of $-1.2 \ cm$ in the negative z direction as shown in figure 4.14. This value increases to $-2 \ cm$ if we decrease the stiffness to $k_1 = 1.8 * 10^5 \ N/m$ with same value of k_2 as shown in figure 4.15.
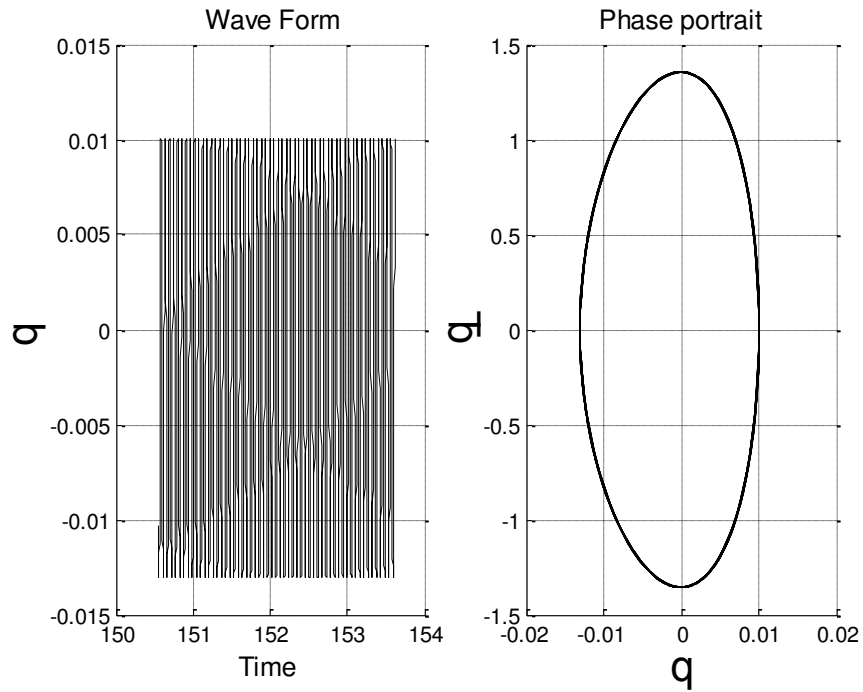
Figure 4.14 Time history and phase portrait for transverse vibration at e=2 cm, k₁=8*10^5 , k₂=10 k₁

In-periodicity continues to increase with decreasing the stiffness of the curved path support.

When the stiffness is less than $k_1 = 1.5 * 10^5 \ N/m$ the response increases dramatically

to $7 \ cm$ as shown in figure 4.16.
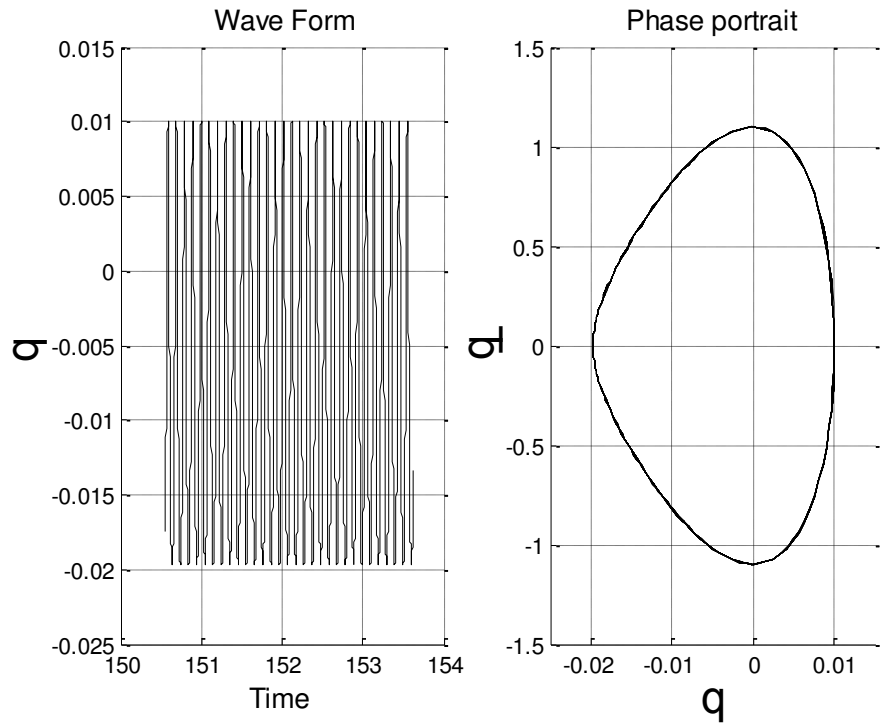
Figure 4.15 Time history and phase portrait for transverse vibration at e=2 cm , k_1=1.8*10^5 , k_2=10 k_1
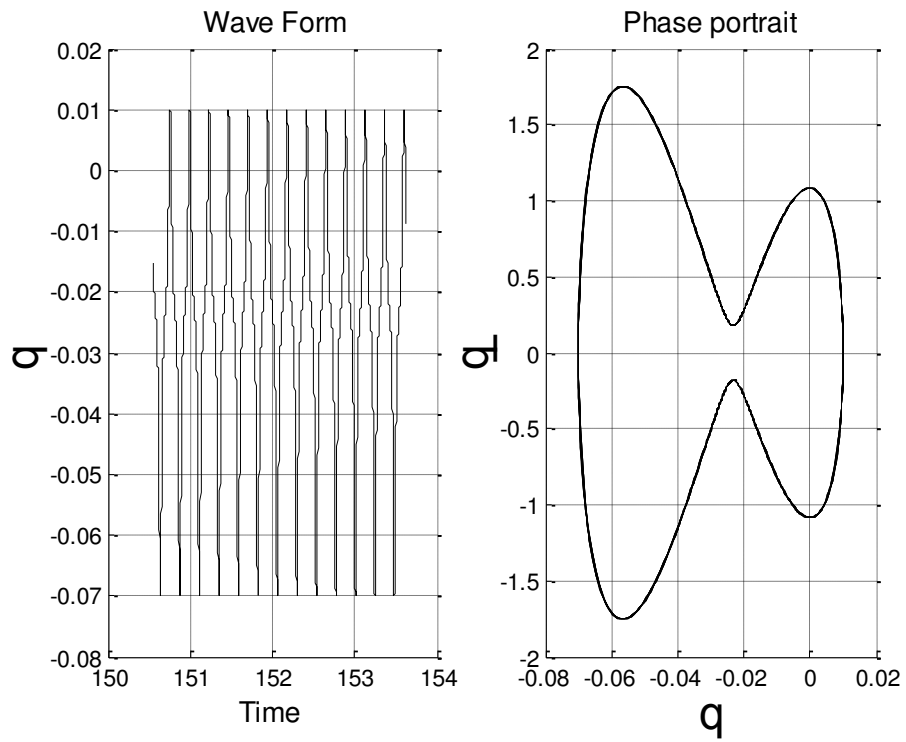
Figure 4.16 Time history and phase portrait for transverse motion at e=2 cm , k_1=1.5*10^5 , k_2=10 k_1

52

CHAPTER 5

Forced vibration of axially moving beam moving in a

curved path

Let us consider a simply supported axially moving beam following a curved path, with the properties shown in Table 4.1.

The curved path is assumed to be a sinusoidal and have an amplitude between 1 and 2 cm. The curved path is considered as an elastic foundation with a combination of linear and nonlinear stiffness coefficients. The beam is traveling axially at a speed of $v = 1m/s$ and subjected to an axial tension of $P = 100\ N$. There is also an external force acting on the surface of the beam in the transverse direction $f = F\cos(\Omega\ t)$.

In this chapter, we study forced vibration of the beam. Section 5.1 includes frequency response curves for primary resonance excitation and show the effect of changing system's parameters. In section 5.2 to 5.5 we analyze the dynamic response of the system through time history, Phase portrait, Poincaré section and bifurcation diagrams. We consider three cases: primary resonance, sub-harmonic and super-harmonic resonances.

5.1. Frequency response curves

The equation of motion of forced vibration reads as

$$\ddot{q}_1 + 2\,\mu\,\dot{q}_1 + a\,q_1 + b\,q_1{}^2 + d\,q_1{}^3 = F\cos\,(\omega\,t) \tag{5.1}$$

In order to derive the frequency response equation, the harmonic balance method [47] is implemented to the second order time domain equation (5.1) where F is the amplitude of the external force and ω is the excitation frequency. Note that the equation describes the first mode of vibration.

The harmonic balance method is used to determine the approximate periodic solutions of nonlinear differential equations. If a periodic solution does exist, it may be sought in the form of a Fourier series, whose coefficients are determined by requiring the series to satisfy the equation of motion. However, in order to avoid solving an infinite system of algebraic equations, it is better to approximate the solution by finite sums of trigonometric functions, i.e.

$$q(t) = \bar{a}\,\sin\,(\omega\,t) + \bar{b}\,\cos\,(\omega\,t) \tag{5.2}$$

Substituting equation (5.2) into the governing equation (5.1), we get

$$
\begin{aligned}
\left[-\bar{a}\,\omega^2\sin\,(\omega\,t) - \bar{b}\,\omega^2\cos\,(\omega\,t)\right] + \mu\left[\bar{a}\,\omega\,\cos\,(\omega\,t) - \right. \\
\left. \bar{b}\,\omega\,\sin\,(\omega\,t)\,\right] + a\left[\bar{a}\,\sin\,(\omega\,t) + \bar{b}\,\cos\,(\omega\,t)\right] + \\
b\left[\bar{a}\,\sin\,(\omega\,t) + \bar{b}\,\cos\,(\omega\,t)\right]^3 = F\cos\,(\omega\,t)
\end{aligned}
\tag{5.3}
$$

Equating the coefficients of each sin (ωt) terms to zero, and the coefficients of each cos (ωt) terms to F, leads to two algebraic equations. We ignore the second and third-order harmonic terms $(2 \omega t)$, $(3 \omega t)$ and concentrate on the fundamental frequency

$$- \bar{a}\,\omega^2 - 2\,\mu\,\bar{b}\,\omega + a\,\bar{a} + \frac{3}{4}d\,\bar{a}\left(\bar{a}^2 + \bar{b}^2\right) = 0$$

$$- \bar{b}\,\omega^2 + 2\,\mu\,\bar{b}\,\omega + a\,\bar{b} + \frac{3}{4}\,d\,\bar{b}\left(\bar{a}^2 + \bar{b}^2\right) = f$$

(5.4)

Define the amplitude of oscillation $A = \sqrt{\bar{a}^2 + \bar{b}^2}$ and substitute it into equations (5.4), square both of the resulted equations to get the frequency response relation between frequency (ω) and amplitude of oscillation (A)

$$A^2 \left(\frac{9}{16}\,A^4 d^2 + \frac{3}{2}\,A^2 d\,a - \frac{3}{2}\,A^2 d\,\omega^2 + a^2 - 2a\omega^2 + m^2\omega^2 + \omega^4\right) = f^2 \qquad (5.5)$$

Simplifying equation (5.5), we get

$$\left[\omega^4 - \left(\frac{3}{2}d\,A + 2a - \mu^2\right)\omega^2 + \left(\frac{3}{4}d\,A + a\right)^2\right] = \left(\frac{f}{A}\right)^2 \qquad (5.6)$$

By solving equation (5.6) we get the frequency response curve for the system. Figure 5.1 shows a linear frequency curve in which we observe that the curve is vertical and the maximum amplitude occurs at a frequency equals to the fundamental frequency. The effect of nonlinear terms in the transverse vibration equation bends the curve away from the linear case as shown in figure 5.2.
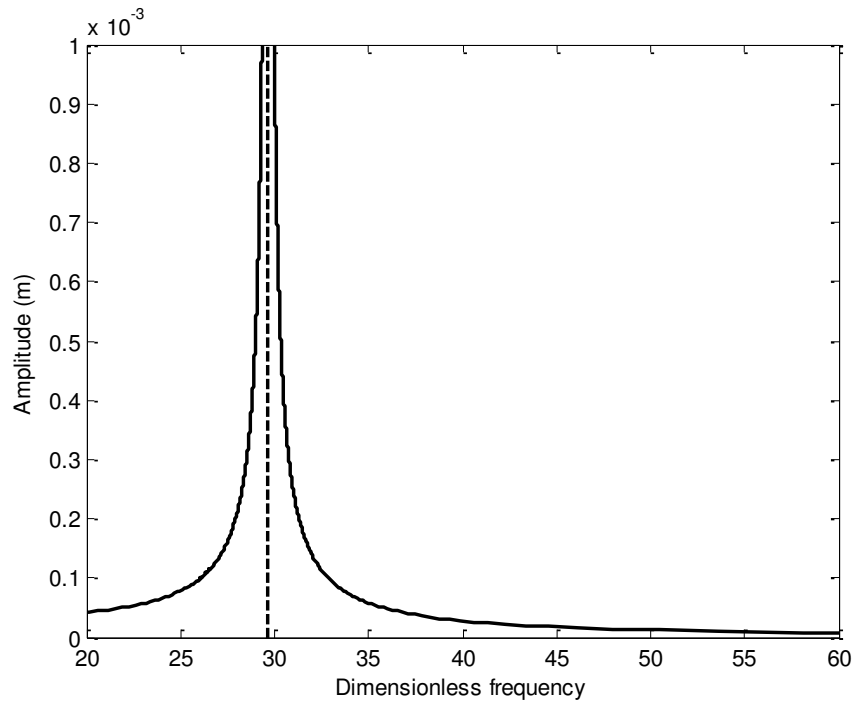
Figure 5.1 Frequency response curve of linear vibration, at e=1 cm
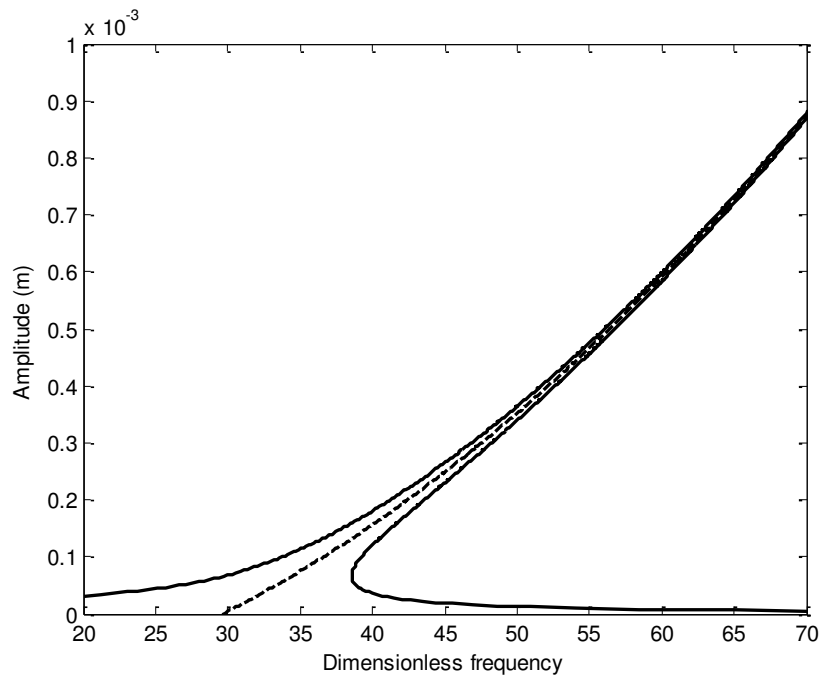
Figure 5.2 Frequency response curve of nonlinear vibration, at e=1 cm

56

The dashed lines in figures 5.1 and 5.2 are called the "Backbone" curves which represent the free vibration frequency curve and it is independent of the force amplitude or the damping coefficient [48].

If we compare the nonlinear and linear vibrations of the system in terms of frequency response curves figure 5.1 and 5.2, respectively, we realize that multi solutions exist at some specific ranges in the forced vibration curve [figure 5.1], for example, the system has three solutions at a frequency equals to 55.

The effect of damping on the frequency response is shown in figure 5.3. As damping increases, the maximum amplitude decreases, while the overall frequency response profile is maintained.
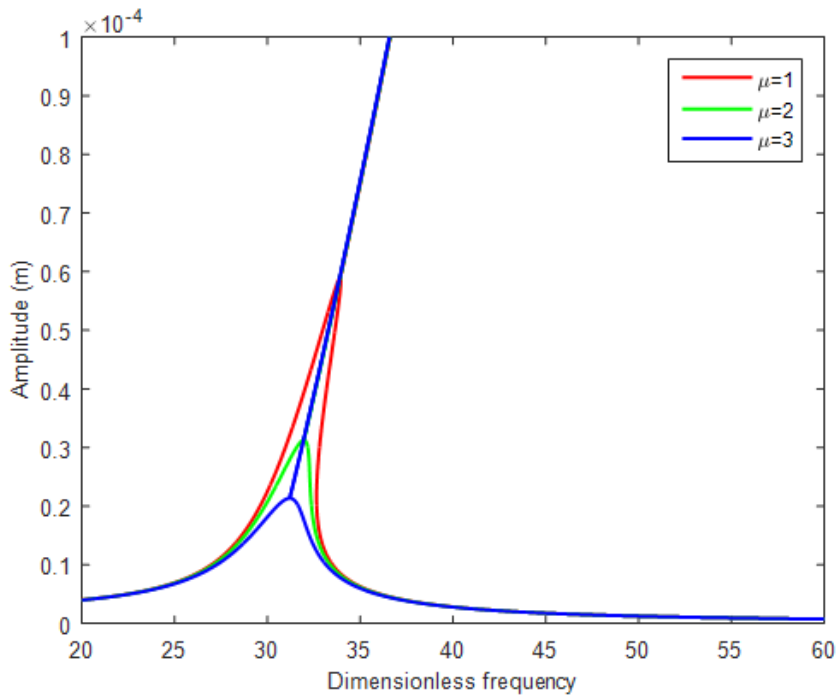
Figure 5.3 Frequency response curves at different damping coefficients, at e=1 cm

Figure 5.4 shows the effect of axial speed on the frequency response curve. By increasing the axial speed we realize a tendency toward nonlinear hardening effect in the system. In such behavior, increasing amplitude, results in increasing the resonance frequency. The response curve becomes asymmetric and leans towards higher frequencies.
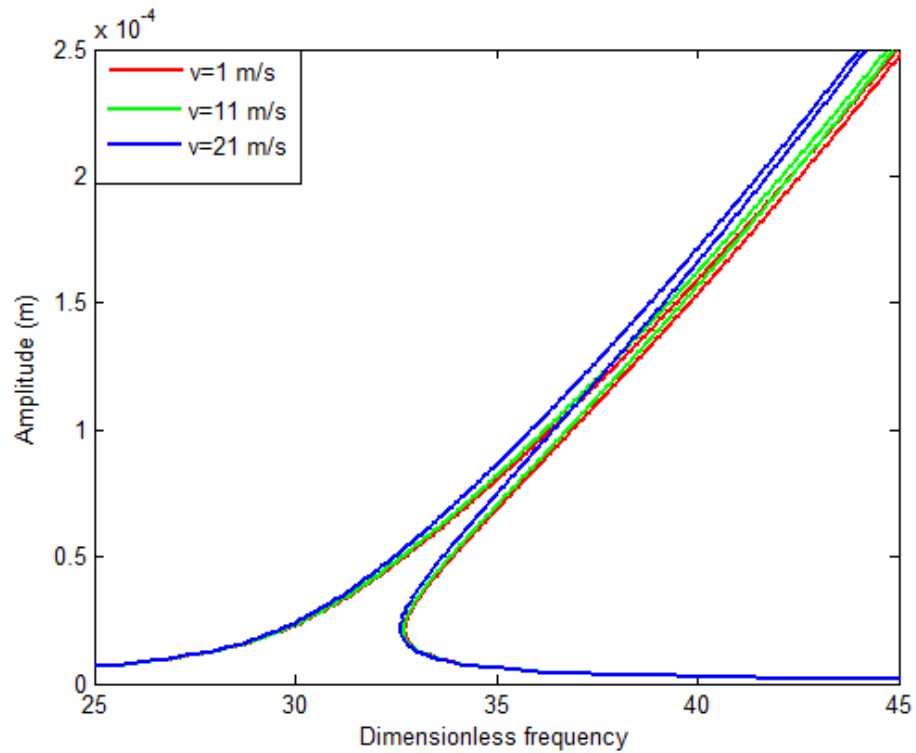
Figure 5.4 Frequency response curves at different axial speed, at e=1 cm

Figure 5.5 shows the effect of amplitude of the excitation force. It is noted that the higher force amplitude results in a higher vibration amplitude over the entire frequency spectrum.
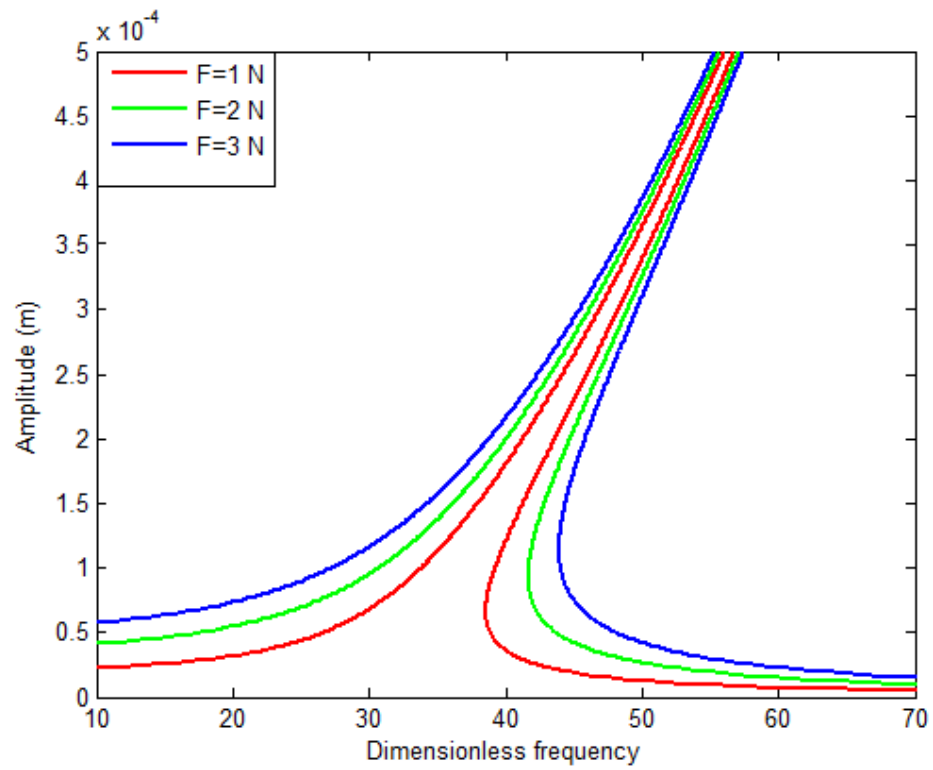
Figure 5.5 Frequency response curves at different force amplitudes, at e=1 cm

5.2. Dynamic response

In this section, we investigate the response of an axially moving beam following a curved path subjected to distributed-harmonic external force excitation. We assume that the transverse harmonic excitation is uniform over the length of the beam. The excitation frequency equals to or multiplier of the fundamental frequency of the first vibration mode.

It is appropriate to define some of the terminology used in the literature concerning nonlinear resonances. Consider a distributed parameter system with natural frequencies ω_n, where n is the mode number. The system is subjected to an external harmonic excitation of frequency Ω . A primary resonance of the nth mode occurs if the excitation frequency is close to the natural frequency of that mode (i.e., $\Omega \cong \omega_n$). A sub-harmonic resonance of the order $1/k$ of the nth mode occurs if $\Omega \cong k\,\omega_n$, where k is an integer. On the other hand, a super-harmonic resonance of order k of the nth mode occurs if $\Omega \cong \omega_n/k$ [44].

5.2.1. Poincaré Section

Poincaré section consists of a 2D plane that intersects the steady-state trajectories, sometimes referred to as the attractor, converting a continuous flow into a discrete time mapping. By observing the distribution of the discrete points on the Poincaré section, we can identify system's behavior.

The trajectory, or orbit, of an object x is sampled periodically, as indicated by the squared section in figure 5.6. The rate of change for the object is determined for each intersection of its orbit with the section. This set of values can then be used to analyze the long term stability of the system [49].
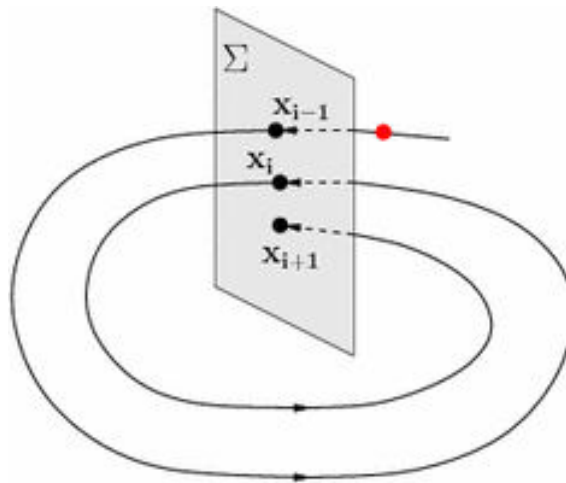

Figure 5.6 Poincare´ section illustration, periodic orbit cross the section [50]

The red point x_{i-1} is the start of original cycle of the system, called the limit cycle of the system, since the system will return to this point every (T) seconds or the period. In contrary to the case of bifurcation or chaos, every period of oscillation (T) the object x will cross

different points in the plane, which will generate a "randomly" distributed points in the displacement speed plane.

5.2.2. Bifurcation diagrams

In the nonlinear systems, it is possible to have several solutions to a differential equation. The number of solutions depends mainly on the parameters that describe the system, however, a small change in any of these parameters may lead to a significant change in the number of solutions and the nature of them as well. That is what is called the "sensitivity" of the system to its parameter's change.

Because the qualitative dynamic behavior of a system changes with the parameter variations, a global description of the system involves the knowledge of all possible behaviors for several parameter values. The bifurcation diagram is a graphical representation of sampled attractors in a Poincaré section and provides a good visual summary of the transitions between different types of motion that can occur when one parameter of the system is varied. This provides an easy identification method of how the system's qualitative behavior changes. A typical bifurcation diagram has a horizontal axis that corresponds to the varring parameter (force, stiffness, speed, etc.) and a vertical axis that corresponds to the sampled steady-state values of one of the system's variables. A large number of data samples are captured using a Poincaré section for each value of the chosen bifurcation parameter and plotted in the bifurcation diagram. By this method we can observe the evolution of the solution as the bifurcation parameter is changed.

Many phenomena are observed in such diagram. Jump phenomena appear as a sudden change in the path of oscillation or a discontinuity in the bifurcation diagram. Some systems are jumping several times as the bifurcation parameter is changed, or a switching behavior of the system from one solution to another.

5.3. Primary resonance excitation ($\Omega = \omega$)

We set the frequency of the excitation external force to a fundamental frequency of the system, which depends on system's parameters as mentioned in chapter 4. The bifurcation diagram is constructed for a straight axially moving beam as shown in figure 5.7 to examine system's response. We consider the external force amplitude as a bifurcation parameter. A quick look at the bifurcation diagram indicates that the system gives one solution for force ranges up to around $6\ N$, and then the diagram starts to bifurcate, generating multiple solutions.
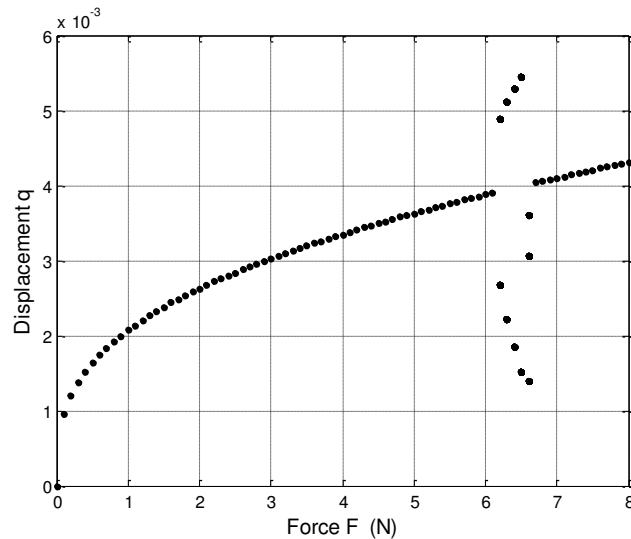
Figure 5.7 bifurcation diagram at primary resonance, at e=0

In contrast, Figure 5.8 shows the bifurcation diagram for the axially moving beam following a curved path, with an amplitude of curvature of 1 mm. In this case, the diagram starts bifurcation earlier when the force amplitude is about 2 N. The Force-displacement diagram exhibits many types of bifurcations, the response undergoes period four bifurcation at force amplitude 2 N, period doubling bifurcation around 3 N and 6 N force amplitudes.
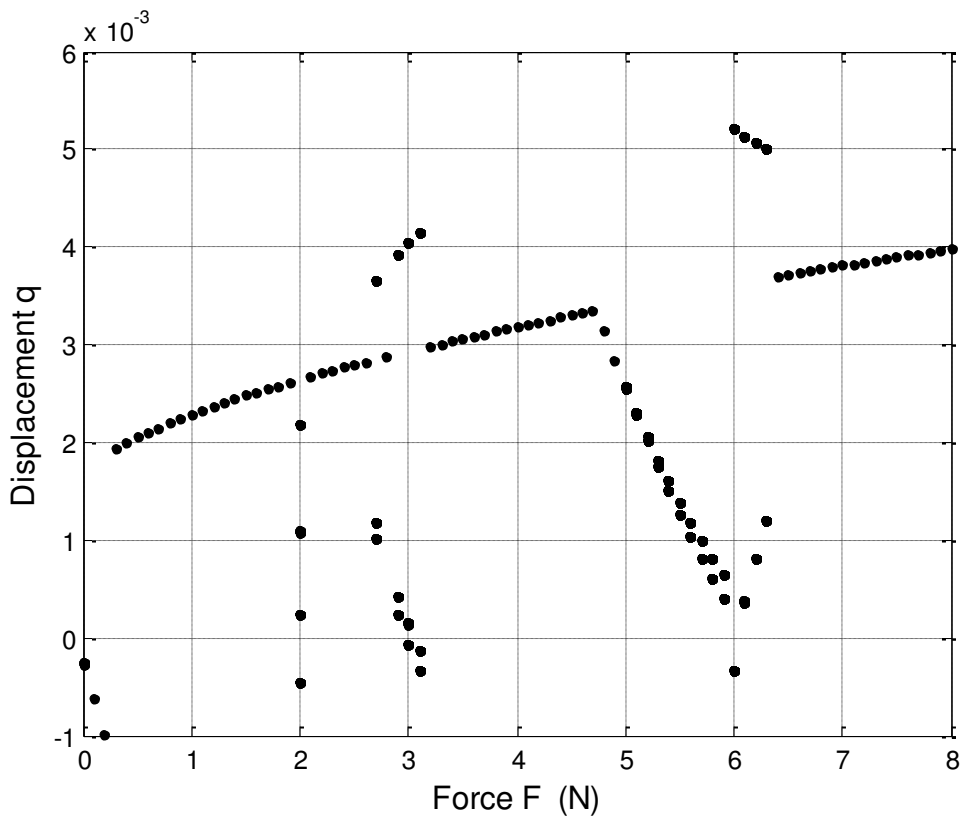
Figure 5.8 bifurcation diagram at primary resonance, at e=1 mm

Figure 5.9 shows the phase portrait, the Poincare´ section and the time history for a period one oscillation at $F = 0.4\ N$ for the axially moving beam with an amplitude of curvature of 1 mm. It is clear that both wave form and phase portrait shows typical characteristics of a periodic motion. Increase of the excitation force amplitude to 2 N for the beam with the

same amplitude of curvature of 1 mm results in a period four bifurcation as shown in figure 5.10. The phase portrait has four different cycles and the wave form has many different amplitudes and frequencies compared to figure 5.9.
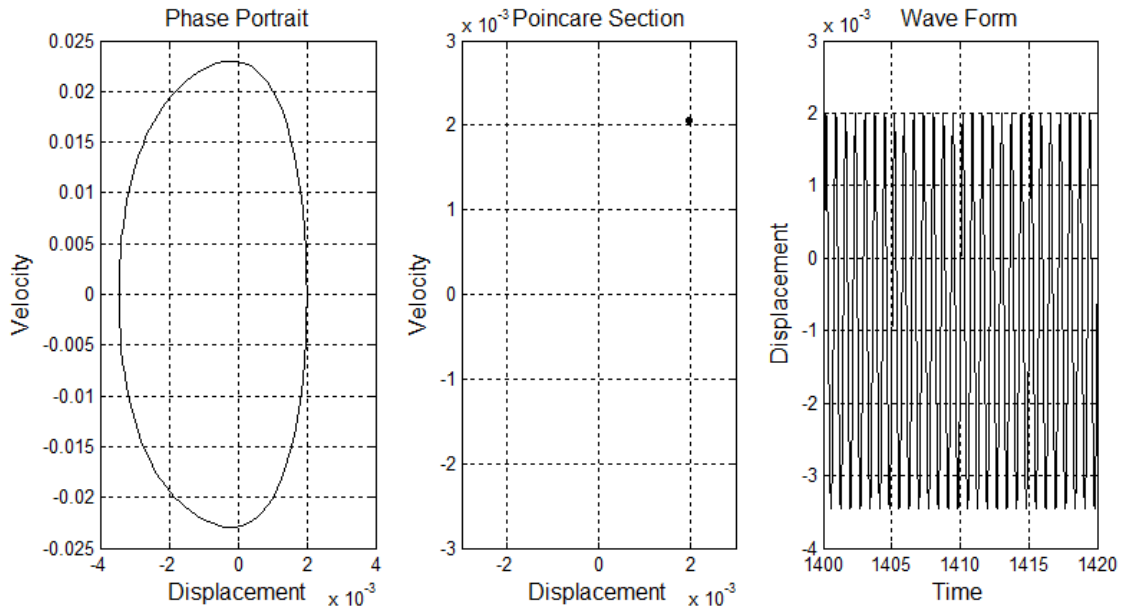
Figure 5.9 Phase portrait, Poincaré section and time history at primary resonance for $F = 0.4\ N$, at e=1 mm
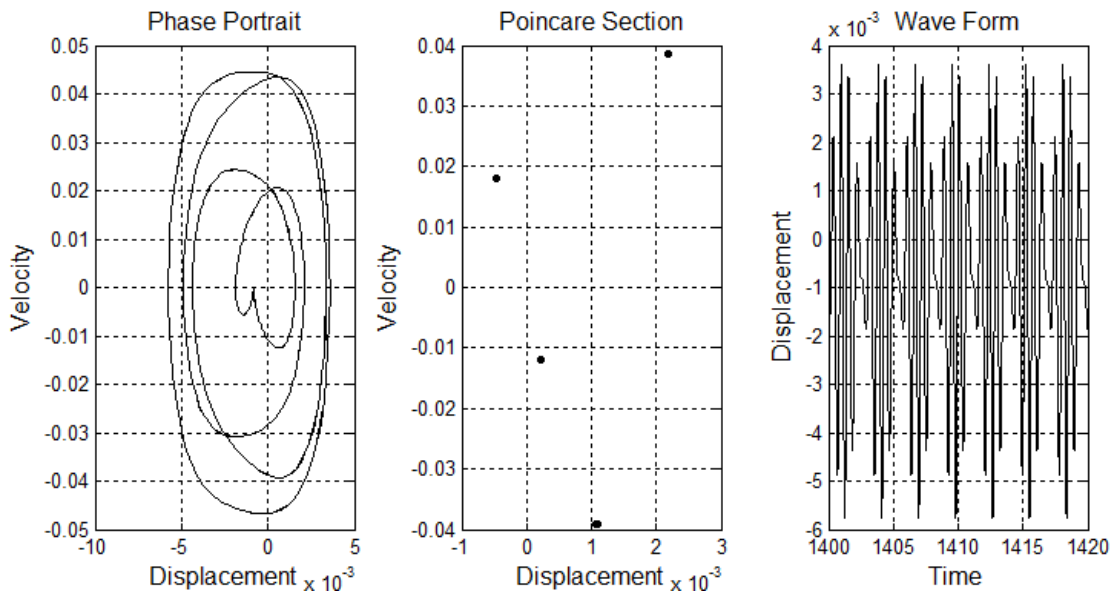
Figure 5.10 Phase portrait, Poincaré section and time history at primary resonance for $F = 2\ N$, at e=1 mm

5.4. Sub-harmonic resonance excitation ($\Omega = 2\ \omega$)

The frequency of the external force is set to double of the fundamental frequency of the system. Let us make a comparison between two cases: axially moving straight beam and axially moving beam following curved path with amplitude of 1 mm in Figure 5.11 and 5.12, respectively. For axially moving straight beam, there is only one solution up to 4.6 N force amplitude in which system has a period- five motion and another bifurcation around 7 N force amplitude. While the curvature causes the system' bifurcation to occur earlier at 3 N force amplitudes, and has another two bifurcations at 5 N and 7 N force amplitudes.
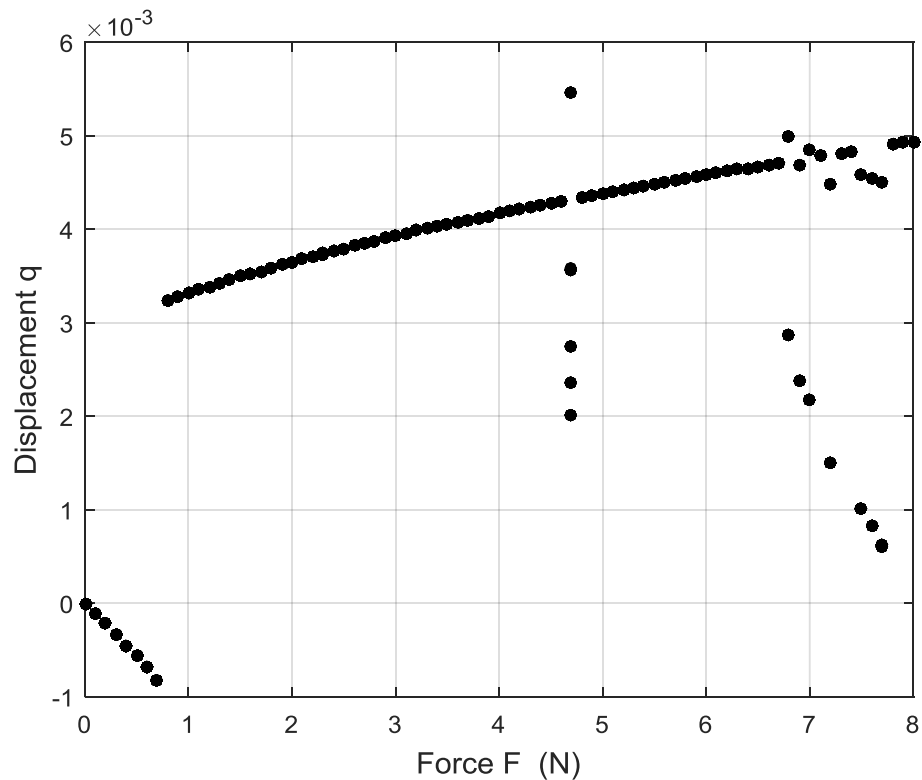
Figure 5.11 bifurcation diagram at sub-harmonic resonance, at e=0
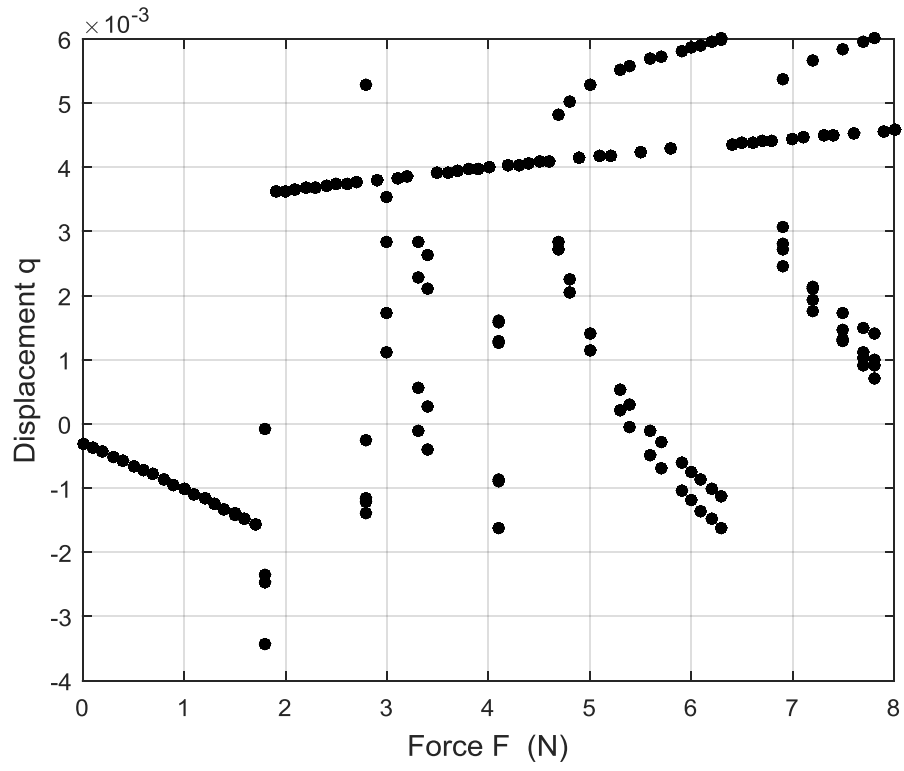
Figure 5.12 bifurcation diagram at sub-harmonic resonance, at e=1 mm

5.5. Super-harmonic resonance excitation ($\Omega = 0.5\ \omega$)

The frequency of the external force is set to half of the natural frequency of the system. Figure 5.13 shows the bifurcation diagram for axially moving straight beam. The Force-displacement diagram exhibits one jump when the force amplitude = 5.2 N, and does not show any bifurcation until F= 8 N.
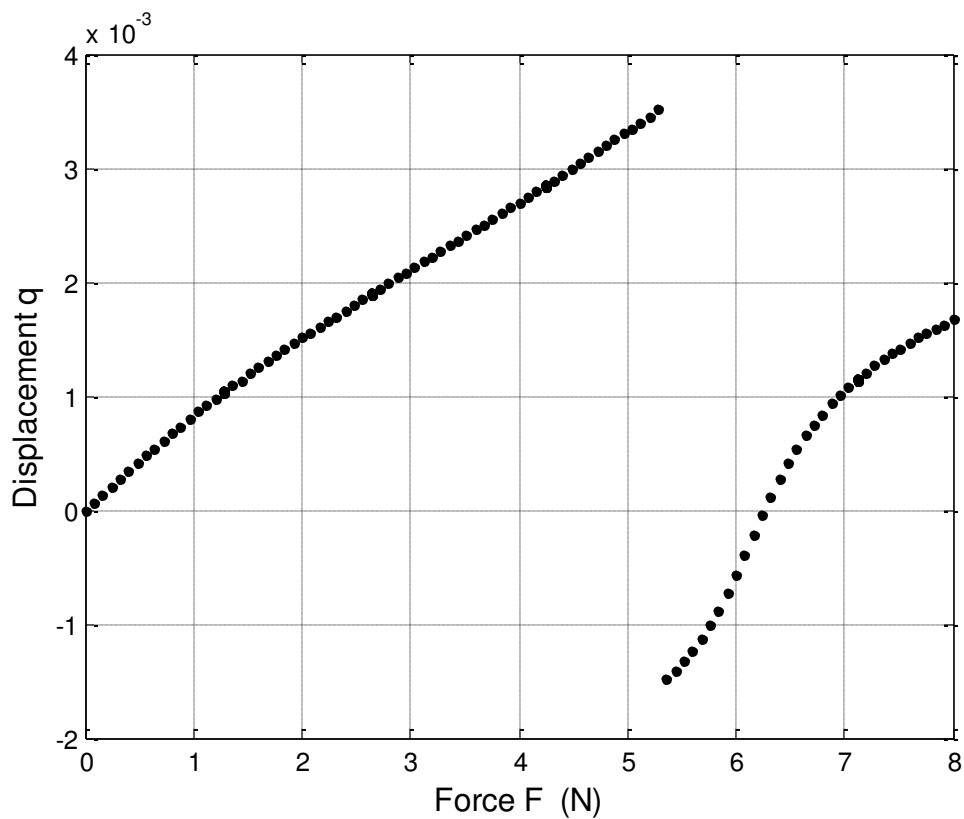
Figure 5.13 bifurcation diagram at super-harmonic resonance, at e=0

For the case of axially moving beam following a curved path with amplitude of 1 mm, the bifurcation diagram shows a jump at F=1.2 N, and a double period bifurcation at 4.2 N as shown in figure 5.14.
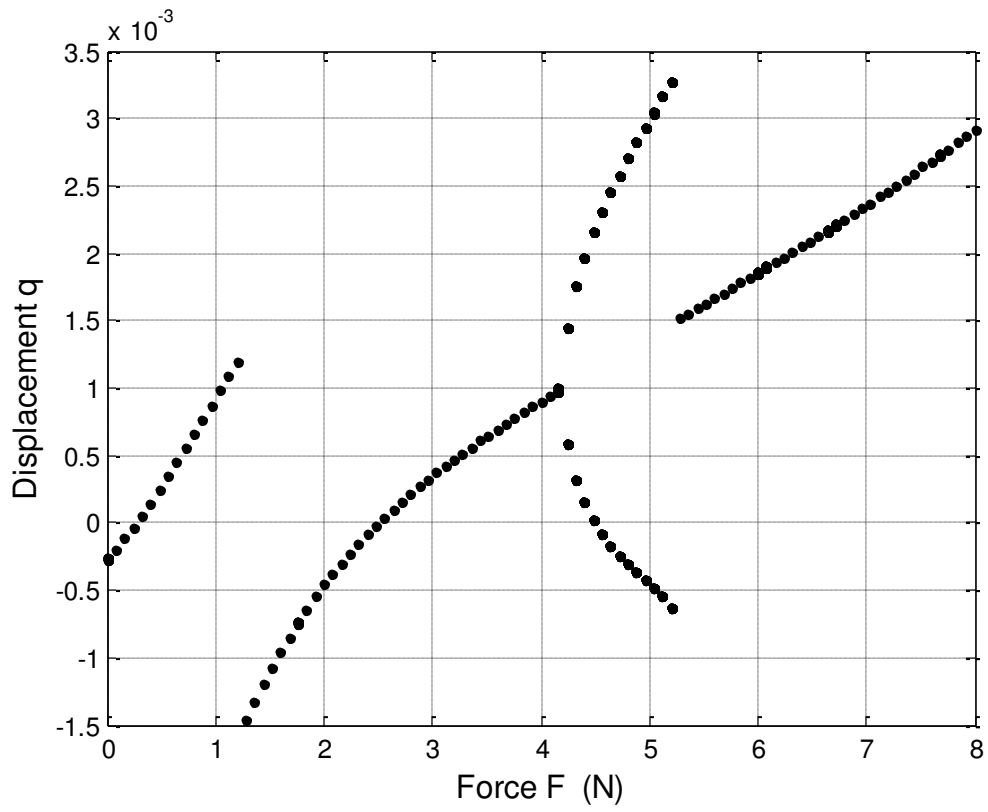
Figure 5.14 bifurcation diagram at super-harmonic resonance, at e=1 mm

CHAPTER 6

Conclusion and Future Outlook

6.1. Conclusion

Equations of motion for an axially moving beam following a curved path was derived using Hamilton principle and then Galerkin's method was used to discretize the coupled equations of motion. We studied free vibration of the beam and examined the effect of system parameters on the natural frequency of the first mode shape vibration.

From the results obtained, considering the vibration of an axially moving beam resting on an elastic curved support, the effect of curvature produced an in-periodicity appears in the system's response as an increase in the downward displacement of beam vibration. The special case of vibration of axially moving straight beam exhibited equal oscillations up and down around the horizontal neutral line.

The natural frequency of an axially moving beam travelling on a curved elastic support was higher than the natural frequency of its straight counterpart beam. This increase was due to new terms introduced to the model by path curvature and linear and nonlinear stiffnesses of the supports. The fundamental frequency increased dramatically with slight increase in elastic support curvature.

Forced vibration of the beam was also studied in three cases: primary resonance, sub-harmonic resonance and super-harmonic resonance excitations. The forced vibration of an axially moving beam on a curved elastic support exhibited many types of bifurcation, the response undergone period doubling bifurcation, period four bifurcation and many jumps. The effect of support curvature was shown to cause the system to start bifurcation very earlier compared with the case of an axially moving beam resting on a straight elastic support.

6.2.   Future Recommendations

Following are recommended potential extensions for future work based on the conclusions reached during this investigation:

1- Studying the model of a viscoelastic beam, to include viscoelastic thin films, paper sheets and PET sheets.

2- Extending the model into micro scale to include applications of printed electronic circuits and other micro-level applications.

3- Studying different configurations of the moving beam, by changing material, geometry and system's parameter.

4- Deriving exact relation between speed and tension in roll to roll systems. And examine the effect of curvature on that system.

References

[1] "http://clearmetalsinc.com/technology/" [Accessed: 12 - Oct 2014].

[2] "http://www.substech.com/dokuwiki/doku.php?id=manufacturing_bi-metal_strips_for_copper_bearings" [Accessed: 7 - Jul 2014].

[3] "https://www.converteraccessory.com/products/wrinkle/ws.php" [Accessed: 17 - Sep 2014].

[4] "http://www.healthista.com/fitness-trends-2015-woodway-curve-2/" [Accessed: 26 - Mar 2014].

[5] A. Kulachenko, P. Gradin, and H. Koivurova, "Modelling the dynamical behaviour of a paper web. Part II" *Computers and Structuers*, vol. 85, no. 3–4, pp. 148–157, Feb. 2007.

[6] C. D. Mote, "On the Nonlinear Oscillation of an Axially Moving String" *Journl of Applied Mechanics*, vol. 33, no. 2, p. 463, 1966.

[7] Vincent Gassmann, Domnique Knittel, Prabhakar R. Pagilla, and Marie-Ange Bueno, "H∞ unwinding web tension control of a strip processing plant using a pendulum dancer" *Proceedings of the American Control Conference*, pp. 901–906, 2009.

[8] J. A. Wickert and C. D. Mote, "Classical Vibration Analysis of Axially Moving Continua" *Journal of Applied Mechanics*, vol. 57, no. September 1990, p. 738, 1990.

[9] J. A. Wickert, "Non-linear vibration of a traveling tensioned beam" *International Journal of Non-Linear Mechanics*, vol. 27, no. 3, pp. 503–517, May 1992.

[10] C. D. Mote, "A study of band saw vibrations" *Journal of the Franklin Institute*, vol. 279, pp. 430–444, 1965.

[11] G. Chakraborty, A. K. Mallik, and H. Hatwal, "Non-linear vibration of a travelling beam" *International Journal of Non-Linear Mechanics*, vol. 34, no. April 1998, pp. 655–670, 1999.

[12] H. R. Öz and M. Pakdemirli, "vibrations of an axially moving beam with time-dependent velocity" *International Journal of Non-Linear Mechanics*, vol. 36, pp. 107–115, 1999.

[13] H. R. Öz M. Pakdemirli and H. Boyaci "Non-linear vibrations and stability of an axially moving beam with time-dependent velocity" *Mechanism and Machine Theory*, vol. 67, pp. 1–16, 2001.

[14] F. Pellicano and F. Vestroni, "Nonlinear Dynamics and Bifurcations of an Axially Moving Beam" *Journal of Vibration and Acoustics*, vol. 122, no. 1, p. 21, 2000.

[15] Li-Q. Chen, Xiao-Dong Yang and Chang-Jun Cheng, "Dynamic stability of an axially accelerating viscoelastic beam" *European Journal of Mechanics - A/Solids*, vol. 23, no. 4, pp. 659–666, Jul. 2004.

[16] Mergen H. Ghayesh and Sara Balar, "Non-linear parametric vibration and stability of axially moving visco-elastic Rayleigh beams" *International Journal of Solids and Structures*, vol. 45, no. 25–26, pp. 6451–6467, Dec. 2008.

[17] Li-Qun Chen and Hu Ding, "Steady-State Transverse Response in Coupled Planar Vibration of Axially Moving Viscoelastic Beams" *Journal of Vibration and Acoustics*, vol. 132, no. 1, p. 011009, 2010.

[18] Hu Ding and Li-Qun Chen, "Galerkin methods for natural frequencies of high-speed axially moving beams" *Journal of Sound and Vibration*, vol. 329, no. 17, pp. 3484–3494, Aug. 2010.

[19] Mergen H. Ghayesh, "Nonlinear forced dynamics of an axially moving viscoelastic beam with an internal resonance" *International Journal of Mechanical Sciences*, vol. 53, no. 11, pp. 1022–1037, Nov. 2011.

[20] Hu Ding and Li-Qun Chen, "Natural frequencies of nonlinear vibration of axially moving beams" *Nonlinear Dynamics*, vol. 63, pp. 125–134, 2011.

[21] J. L. Huang, R. K. L. Su, W. H. Li, and S. H. Chen, "Stability and bifurcation of an axially moving beam tuned to three-to-one internal resonances" *Journal of Sound and Vibration*, vol. 330, no. 3, pp. 471–485, Jan. 2011.

[22] Mergen H. Ghayesh and Marco Amabili, "Nonlinear dynamics of axially moving viscoelastic beams over the buckled state" *Computers & Structures*, vol. 112–113,

pp. 406–421, Dec. 2012.

[23]   Li-Qun Chen and You-Qi Tang, "Parametric Stability of Axially Accelerating Viscoelastic Beams With the Recognition of Longitudinally Varying Tensions" *Journal of Vibration and Acoustics*, vol. 134, no. 1, p. 011008, 2012.

[24]   Mergen H. Ghayesh, Michael P. Païdoussis, and Marco Amabili, "Subcritical parametric response of an axially accelerating beam" *Thin-Walled Structures*, vol. 60, pp. 185–193, Nov. 2012.

[25]   Hamed Farokhi, Mergen H. Ghayesh, and Marco Amabili, "In-plane and out-of-plane nonlinear dynamics of an axially moving beam" *Chaos, Solitons & Fractals*, vol. 54, pp. 101–121, Sep. 2013.

[26]   Mergen H. Ghayesh and Marco Amabili, "Steady-state transverse response of an axially moving beam with time-dependent axial speed" *International Journal of Non-Linear Mechanics*, vol. 49, pp. 40–49, Mar. 2013.

[27]   Hamideh Seddighi and Hamidreza Eipakchi, "Natural frequency and critical speed determination of an axially moving viscoelastic beam" *Mechanics of Time-Dependent Materials*, vol. 17, pp. 529–541, 2013.

[28]   Mergen H. Ghayesh, Marco Amabili, and Hamed Farokhi, "Two-dimensional nonlinear dynamics of an axially moving viscoelastic beam with time-dependent axial speed" *Chaos, Solitons & Fractals*, vol. 52, pp. 8–29, Jul. 2013.

[29]   Xiao-Dong Yang and Wei Zhang, "Nonlinear dynamics of axially moving beam with coupled longitudinal–transversal vibrations" *Nonlinear Dynamics*, vol. 78, no. 4, pp. 2547–2556, Dec. 2014.

[30]   Krzysztof Marynowski and Tomasz Kapitaniak, "Dynamics of axially moving continua" *International Journal of Mechanical Sciences*, vol. 81, pp. 26–41, Apr. 2014.

[31]   Bamadev Sahoo, L.N. Panda, and Goutam Pohit, "Stability and bifurcation analysis of an axially accelerating beam" *Vibration Engineering and Technology of Machinery, Mechanisms and Machine Science,* vol. 23, 2015.

[32]   S. M. Bağdatli, E. Özkaya, and H. R. Öz, "Dynamics of Axially Accelerating Beams With an Intermediate Support" *Journal of Vibration and Acoustics*, vol.

133, no. 3, p. 031013, 2011.

[33]   Mergen H. Ghayesh, "Stability and bifurcations of an axially moving beam with an intermediate spring support" *Nonlinear Dynamics*, vol. 69, no. 1–2, pp. 193–210, Jul. 2012.

[34]   Mergen H. Ghayesh, "Nonlinear dynamic response of a simply-supported Kelvin–Voigt viscoelastic beam, additionally supported by a nonlinear spring" *Nonlinear Analysis: Real World Applications*, vol. 13, no. 3, pp. 1319–1333, Jun. 2012.

[35]   Mergen H. Ghayesh, Marco Amabili, and Michael P. Païdoussis, "Nonlinear vibrations and stability of an axially moving beam with an intermediate spring support: two-dimensional analysis" *Nonlinear Dynamics*, vol. 70, no. 1, pp. 335–354, Oct. 2012.

[36]   Sungpil Park and Jintai Chung, "Dynamic analysis of an axially moving finite-length beam with intermediate spring supports" *Journal of Sound and Vibration*, vol. 333, no. 24, pp. 6742–6759, Dec. 2014.

[37]   Edward B. Magrab, "Vibration of elastic systems" *Solid Mechanics and its Applications*, vol. 184, 2012, pp. 1–6.

[38]   Erwin Kreyszig, "Advanced Engineering Mathematics " *John Wiley & Sons,* 2006.

[39]   Jerry H. Ginsberg, "Advanced Engineering Dynamics" *Cambridge University Press,* 1995.

[40]   H. R. Öz, M. Pakdemirli, E. Özkaya, and M. Yilmaz, "Non-linear vibration of a slightly curved beam resting on a non-linear elastic foundation" *Journal of Sound and Vibration*, vol. 212, no. 2, pp. 295–309, Apr. 1998.

[41]   Fathi N. Mayoof and Muhammad A. Hawwa, "Chaotic behavior of a curved carbon nanotube under harmonic excitation" *Chaos, Solitons & Fractals*, vol. 42, no. 3, pp. 1860–1867, Nov. 2009.

[42]   J. L. Huang, R. K. L. Su, Y. Y. Lee, and S. H. Chen, "Nonlinear vibration of a curved beam under uniform base harmonic excitation with quadratic and cubic nonlinearities" *Journal of Sound and Vibration*, vol. 330, no. 21, pp. 5151–5164, Oct. 2011.

[43]   Gozde Sarı and Mehmet Pakdemirli, "Vibrations of a Slightly Curved Microbeam Resting on an Elastic Foundation with Nonideal Boundary Conditions" *Mathematical Problems in Engineering*, vol. 2013, pp. 1–16, 2013.

[44]   Ali H. Nayfeh and P. Frank Pai, "Linear and Nonlinear Structural Mechanics" *John Wiley and sons, Inc.* , 2004.

[45]   Sheng-Jiaw Hwang, "Supercritical stability of axially moving materials" *PHD thesis, University of Michigan,* 1991.

[46]   Prabhakar R. Pagilla, Nilesh B. Siraskar, and Ramamurthy V. Dwivedula, "Decentralized Control of Web Processing Lines" *IEEE Transactions on Control Systems Technology*, vol. 15, no. 1, pp. 106–117, Jan. 2007.

[47]   V. Marinca and N. Herisanu, "Nonlinear Dynamical Systems in Engineering" *Springer-Verlag Berlin Heidelberg,* 2011.

[48]   V. K. Astashev, M. Z. Kolovsky, and V. I. Babitsky, "Dynamics and Control of Machines" *Springer Science & Business Media,* 2000.

[49]   Gregory L. Baker and Jerry P. Gollub, "Chaotic Dynamics: An Introduction" *Cambridge University Press,* 1996.

[50]   "http://komputasirobotic.blogspot.com/2013/04/analisis-peta-poincare-poincare-map.html." [Accessed: 22 - Oct 2014].

Appendix

Kinetic energy terms

$$T = \frac{\rho A}{2} \int_0^L \{u_t^2 + 2\,u_t\,v\,(1 + u_x) + v^2\,(1 + u_x)^2 + w_t^2 + 2\,w_t\,v\,w_x + 2\,w_t\,v\,Z_x +$$

$$v^2\,w_x^2 + 2\,v^2\,w_x\,Z_x\,\}\,dx$$

keeping the constant $\frac{\rho A}{2}$ for all terms and plug it later in The Hamilton Principle.

1- $\int_0^L u_t^2 \ dx$

This term will be integrated with respect to time on The Hamilton Principle. But we can

do it now and make the result ready for use without integration.

$$= \int_0^L \int_{t_1}^{t_2} u_t\,u_t \ dt \ dx$$

$$= \int_0^L \left([u_t\,\delta u]\,_{t_1}^{t_2} - \int_{t_1}^{t_2} u_{tt}\,\delta u \ dt \right) dx$$

$$= - \int_{t_1}^{t_2} \int_0^L u_{tt}\,\delta u \ dx \ dt$$

$$= - \int_0^L u_{tt} \ dx$$

2- $\int_0^L 2\,u_t\,v\,(1 + u_x)\,dx$

$$= \int_0^L 2\,v\,u_t \ dx + \int_0^L 2\,v\,u_t\,u_x \ dx$$

77

$$\int_0^L 2\,v\,u_t\,dx = 2\,v\,[u_t\,x]\,\Big\vert_0^L$$

$$\int_0^L 2\,v\,u_t\,u_x\,dx = v\,[u_t\,u]\,\Big\vert_0^L - v\int_0^L u_{tx}\,u\,dx$$

3- $\int_0^L v^2\,(1 + u_x)^2\,dx$

$$= v^2 \int_0^L (1 + 2u_x + u_x^2)\,dx$$

$$v^2 \int_0^L dx = v^2[x]\,\Big\vert_0^L$$

$$v^2 \int_0^L 2u_x\,dx = 2\,v^2[u]\,\Big\vert_0^L$$

$$v^2 \int_0^L u_x u_x\,dx = v^2[u_x\,u]\,\Big\vert_0^L - v^2\int_0^L u_{xx}\,u\,dx$$

4- $\int_0^L w_t^2\,dx$

This term also like the first term will be integrated with respect to time on The Hamilton

Principle. But we can do it now and make the result ready for use without integration.

$$= \int_0^L \int_{t_1}^{t_2} w_t\,w_t\,dt\,dx$$

$$= \int_0^L \left([w_t\,\delta w]\,\Big\vert_{t_1}^{t_2} - \int_{t_1}^{t_2} w_{tt}\,\delta w\,dt \right) dx$$

$$= - \int_{t_1}^{t_2} \int_0^L w_{tt} \, \delta w \, dx \, dt$$

$$= - \int_0^L w_{tt} \, dx$$

5- $\int_0^L 2 \, w_t \, v \, w_x \, dx$

$$= 2 \, v [w_t \, w] \bigg|_0^L - 2 \, v \int_0^L w_{tx} \, w \, dx$$

6- $\int_0^L 2 \, v \, w_t \, Z_x \, dx$

$$= 2 \, v \int_0^L w_t \, Z_x \, dx$$

$$= 2v \, [w_t \, Z] \bigg|_0^L - 2v \int_0^L w_{xt} \, Z \, dx$$

7- $\int_0^L v^2 \, w_x^2 \, dx$

$$= v^2 \int_0^L w_x \, w_x \, dx$$

$$= v^2 [w_x \, w] \bigg|_0^L - v^2 \int_0^L w_{xx} \, w \, dx$$

8- $\int_0^L 2 \, v^2 \, w_x \, Z_x \, dx$

$$= 2 \, v^2 [Z_x \, w] \bigg|_0^L - 2v^2 \int_0^L Z_{xx} \, w \, dx$$

Potential energy terms

$$U = \int_0^L \left[P\,\varepsilon + \frac{1}{2}\,E\,A\,\varepsilon^2 + \frac{1}{2}\,E\,I\,w_{xx}^2 + \frac{1}{2}\,k_1\,w^2 + \frac{1}{2}\,k_2\,w^4 \right] dx$$

1- $\int_0^L P\,\varepsilon\,dx$

$= P \int_0^L \left(u_x + \frac{1}{2}w_x^2 + w_x\,Z_x \right) dx$

$$P \int_0^L u_x\,dx = P[u]\,_0^L$$

$$\frac{P}{2}\int_0^L w_x w_x\,dx = \frac{P}{2}\,[w_x\,w]\,_0^L - \frac{P}{2}\int_0^L w_{xx}\,w\,dx$$

$$P \int_0^L w_x\,Z_x\,dx = P[Z_x\,w]\,_0^L - P\int_0^L Z_{xx}\,w\,dx$$

2- $\frac{1}{2}\mathrm{EA}\int_0^L \varepsilon^2\,dx$

$= \frac{\mathrm{EA}}{2}\int_0^L \left(u_x + \frac{1}{2}w_x^2 + w_x\,Z_x \right)\left(u_x + \frac{1}{2}w_x^2 + w_x\,Z_x \right) dx$

$= \frac{\mathrm{EA}}{2}\int_0^L u_x\left(u_x + \frac{1}{2}w_x^2 + w_x\,Z_x \right) dx + \frac{\mathrm{EA}}{2}\int_0^L \frac{w_x^2}{2}\left(u_x + \frac{1}{2}w_x^2 + w_x\,Z_x \right) dx +$
$\frac{\mathrm{EA}}{2}\int_0^L w_x\,Z_x\left(u_x + \frac{1}{2}w_x^2 + w_x\,Z_x \right) dx$

$\frac{\mathrm{EA}}{2}\int_0^L u_x\left(u_x + \frac{1}{2}w_x^2 + w_x\,Z_x \right) dx = \frac{\mathrm{EA}}{2}\left[\left(u_x + \frac{1}{2}w_x^2 + w_x\,Z_x \right) u \right]_0^L - \frac{\mathrm{EA}}{2}\int_0^L \left(u_x + \frac{1}{2}w_x^2 + w_x\,Z_x \right)_x u\,dx$

$$\frac{EA}{2}\int_0^L \frac{w_x}{2}\, w_x \left(u_x + \frac{1}{2}w_x^2 + w_x\, Z_x\right) dx = \frac{EA}{2}\left[\left(u_x + \frac{1}{2}w_x^2 + w_x\, Z_x\right)w_x\ \frac{w}{2}\right]_0^L -$$
$$\frac{EA}{2}\int_0^L \left[\left(u_x + \frac{1}{2}w_x^2 + w_x\, Z_x\right)w_x\right]_x \frac{w}{2}\, dx$$

$$\frac{EA}{2}\int_0^L w_x\, Z_x \left(u_x + \frac{1}{2}w_x^2 + w_x\, Z_x\right) dx = \frac{EA}{2}\left[\left(u_x + \frac{1}{2}w_x^2 + w_x\, Z_x\right)Z_x\, w\right]_0^L -$$
$$\frac{EA}{2}\int_0^L \left[\left(u_x + \frac{1}{2}w_x^2 + w_x\, Z_x\right)Z_x\right]_x w\, dx$$

3- $\frac{1}{2}\, E\, I \int_0^L w_{xx}^2\, dx$

$$\frac{EI}{2}\int_0^L w_{xx}\, w_{xx}\, dx = \frac{EI}{2}\left[w_{xx}\, w_x\right]_0^L - \frac{EI}{2}\int_0^L w_{xxx}\, w_x\, dx$$

$$\frac{EI}{2}\int_0^L w_{xxx}\, w_x\, dx = \frac{EI}{2}\left[w_{xxx}\, w\right]_0^L - \frac{EI}{2}\int_0^L w_{xxxx}\, w\, dx$$

$$\frac{EI}{2}\int_0^L w_{xx}^2\, dx = \frac{EI}{2}\left[w_{xx}\, w_x\right]_0^L - \frac{EI}{2}\left[w_{xxx}\, w\right]_0^L + \frac{EI}{2}\int_0^L w_{xxxx}\, w\, dx$$

4- $\frac{1}{2}\, k_1 \int_0^L w^2\, dx$

$$= \frac{1}{2}\, k_1 \int_0^L w\, w\, dx$$

5- $\frac{1}{2}\, k_2 \int_0^L w^4\, dx$

$$= \frac{1}{2}\, k_2 \int_0^L w^3\, w\, dx$$

Derivatives of used functions

$$w_x = q_1\, \frac{\pi}{L}\, \cos\left(\frac{\pi x}{L}\right)$$

$$w_{xx} = -q_1\, \left(\frac{\pi}{L}\right)^2 \sin\left(\frac{\pi x}{L}\right)$$

$$w_{xxx} = -q_1\, \left(\frac{\pi}{L}\right)^3 \cos\left(\frac{\pi x}{L}\right)$$

$$w_{xxxx} = q_1\, \left(\frac{\pi}{L}\right)^4 \sin\left(\frac{\pi x}{L}\right)$$

$$u_x = q_2 \frac{\pi}{L} \cos(\frac{\pi x}{L})$$

$$u_{xx} = -q_2 \left(\frac{\pi}{L}\right)^2 \sin(\frac{\pi x}{L})$$

$$Z_x = e \frac{\pi}{L} \cos(\frac{\pi x}{L})$$

$$Z_{xx} = -e \left(\frac{\pi}{L}\right)^2 \sin(\frac{\pi x}{L})$$

$$w_t = \dot{q}_1 \sin(\frac{\pi x}{L})$$

$$w_{tt} = \ddot{q}_1 \sin(\frac{\pi x}{L})$$

$$w_{tx} = \dot{q}_1 \frac{\pi}{L} \cos(\frac{\pi x}{L})$$

$$u_t = \dot{q}_2 \sin(\frac{\pi x}{L})$$

$$u_{tt} = \ddot{q}_2 \sin(\frac{\pi x}{L})$$

$$u_{tx} = \dot{q}_2 \frac{\pi}{L} \cos(\frac{\pi x}{L})$$

$$\int_0^1 \sin^2(\pi x)\ dx = \frac{1}{2}$$

$$\int_0^L \sin(\pi x) \sin(2\pi x)\ dx = 0$$

$$\int_0^L \sin(\pi x) \cos(\pi x)\ dx = 0$$

$$\int_0^1 \sin^2(\pi x) \cos^2(\pi x)\ dx = \frac{1}{8}$$

$$\int_0^1 \sin^4(\pi x)\ dx = \frac{3}{8}$$

Vitae

Name   : Aalim Motasim Aalim Mustafa

Nationality   : Sudanese

Date of Birth   :10/13/1988

 Email   : aalim.motasim@hotmail.com

Address   : Sudan – Khartoum – Suba Sharg – Square 2

Academic Background:

- M.Sc. Mechanical Engineering: King Fahd University of Petroleum and Minerals (KFUPM), Dhahran, Saudi Arabia 2015
- B.S Mechanical Engineering: University of Khartoum

  Khartoum, Sudan 2010

Research interest: System dynamics, vibration and control.

Experience:

- Mechanical Design Engineer 2012 – 2013

  CST (Center Of Sensors Technology)

  Khartoum, Sudan

- Teaching Assistant 2010 – 2012

  Eljeraf Shareg College

  Khartoum, Sudan

- Teaching Assistant 2010 – 2011

  University of Khartoum

  Khartoum, Sudan

Honors & Awards:

- KFUPM's Scholarship - Full scholarship 2013
- Sudan Engineering Society Award for the best performance at graduation project - Mechanical Engineering 2010
- Scientific Organization for Engineering and Computer Students' Award for the best graduation project - Mechanical Engineering 2010